AD 749282

INTERACTION BETWEEN AMORPHOUS SEMICONDUCTOR THIN FILM AND ELECTRON BEAM

Arthur C. M. Chen and A. M. Wang

General Electric Corporate Research and Development
Schenectady, New York
Telephone: AC518-346-8771

Semiannual Technical Report No. 1, August 30, 1972

Contract No: DAH[illegible]04-72-C-0016
ARPA Order No: 1562, Am. 1
Program Code No: 61101D

Period of Contract: Feb. 7, 1972 to Feb. [illegible], 1973

Amount of Grant/Contract $31,882

Prepared For

U.S. Army Research Office
Durham, North Carolina 27706

and

Advanced Research Projects Agency
Arlington, Virginia 22209

D D C
OCT 2 1972

Reproduced by
NATIONAL TECHNICAL
INFORMATION SERVICE
U S Department of Commerce
Springfield VA 22151

Approved for public release; distribution unlimited

The views and conclusions contained in this document are those of the authors and should not be interpreted as necessarily representing the official policies, either expressed or implied, of the Advanced Research Projects Agency or the U.S. Government

SRD-72-119

45

UNCLASSIFIED
Security Classification

DOCUMENT CONTROL DATA - R & D

(Security classification of title, body of abstract and indexing annotation must be entered when the overall report is classified)

1. ORIGINATING ACTIVITY *(Corporate author)*
General Electric Company
Corporate Research and Development Center, K1
Schenectady, New York

2a. REPORT SECURITY CLASSIFICATION
Unclassified

2b. GROUP

3. REPORT TITLE
INTERACTION BETWEEN AMORPHOUS SEMICONDUCTOR THIN FILM AND ELECTRON BEAM

4. DESCRIPTIVE NOTES *(Type of report and inclusive dates)*
Semiannual Technical Report 1 - February 7, 1972 to August 6, 1972

5. AUTHOR(S) *(First name, middle initial, last name)*
Arthur C. M. Chen
Jish-Min Wang

6. REPORT DATE
August 1972

7a. TOTAL NO. OF PAGES
37

7b. NO. OF REFS
25

8a. CONTRACT OR GRANT NO.
DAHC 04-72-C-0016

b. PROJECT NO.
ARPA Order No. 1562, Am. 1

c.
Program Code No: 61101D

d.

9a. ORIGINATOR'S REPORT NUMBER(S)
SRD-72-119

9b. OTHER REPORT NO(S) *(Any other numbers that may be assigned this report)*

10. DISTRIBUTION STATEMENT
Approved for public release; distribution unlimited.

11. SUPPLEMENTARY NOTES

Reproduced from best available copy.

12. SPONSORING MILITARY ACTIVITY
Advanced Research Projects Agency
via U. S. Army Research Office
Durham, North Carolina 27706

13. ABSTRACT

This is the first semiannual technical report on the research program, Interaction Between Amorphous Semiconductor Thin Film and Electron Beam, sponsored by the U. S. Army Research Office, Durham, North Carolina and the Advanced Research Projects Agency, Arlington, Va. under contract DAHC 04-72-C-0016. The report describes the research conducted during the period Feb. 7, 1972 to Aug. 6, 1972 as well as summarize the research conducted by the investigators on this subject prior to the above period.

The ~~first part of this technical~~ report summarizes ~~our~~ present understanding of the interaction between amorphous semiconductor thin films and electron beam and the potential device and system characteristics of an amorphous semiconductor electron beam memory which exploits this interaction. The feasibility of amorphous semiconductor thin films for storing submicron recordings at high writing speed has been demonstrated. Some studies of the trade offs between the electron beam writing characteristics and the target thermal characteristics by computer simulation are described.

The memory's speed-density capabilities are constraints by the limited beam current, signal detection limitations and acceptable error rates. The resultant speed-density limitations of this memory imposed by the above fundamental physical constraints are derived.

A theory for the memory's modulation efficiency for readout by surface deformation has been derived. The angular dependence of the secondary yield of amorphous semiconductor and Mo has been measured to determine quantitatively the possible modulation efficiency. A special apparatus was built for these measurements.

DD FORM 1 NOV 1473

UNCLASSIFIED
Security Classification

14 KEY WORDS	LINK A ROLE	LINK A WT	LINK B ROLE	LINK B WT	LINK C ROLE	LINK C WT
Interaction						
Amorphous Semiconductors						
Electron Beam Memory System						

INTERACTION BETWEEN AMORPHOUS SEMICONDUCTOR THIN FILM AND ELECTRON BEAM

Arthur C. M. Chen and J. M. Wang

General Electric Corporate Research and Development
Schenectady, New York

Semiannual Technical Report No. 1

August 30, 1972

Approved for public release; distribution unlimited

Prepared For

U. S. Army Research Office
Durham, North Carolina 27706

and

Advanced Research Projects Agency
Arlington, Virginia 22209

TECHNICAL SUMMARY

This is the first semiannual technical report on the research program, Interaction Between Amorphous Semiconductor Thin Film and Electron Beam, sponsored by the U.S. Army Research Office, Durham, North Carolina and the Advanced Research Projects Agency, Arlington, Va. under contract DAHC 04-72-C-0016. The report describes the research conducted during the period Feb. 7, 1972 to Aug. 6, 1972 as well as summarize the research conducted by the investigators on this subject prior to the above period.

The first part of this technical report summarizes our present understanding of the interaction between amorphous semiconductor thin films and electron beam and the potential device and system characteristics of an amorphous semiconductor electron beam memory which exploits this interaction. The feasibility of amorphous semiconductor thin films for storing submicron recordings at high writing speed has been demonstrated. Some studies of the trade offs between the electron beam writing characteristics and the target thermal characteristics by computer simulation are described.

The memory's speed-density capabilities are constraints by the limited beam current, signal detection limitations and acceptable error rates. The resultant speed-density limitations of this memory imposed by the above fundamental physical constraints are derived.

A theory for the memory's modulation efficiency for readout by surface deformation has been derived. The angular dependence of the secondary yield of amorphous semiconductor and Mo has been measured to determine quantitatively the possible modulation efficiency. A special apparatus was built for these measurements.

TABLE OF CONTENTS

Section		Page
	TECHNICAL SUMMARY	ii
	LIST OF ILLUSTRATIONS	
I	INTRODUCTION	1
II	A SYSTEM CONSIDERATION OF AMORPHOUS SEMICONDUCTOR ELECTRON BEAM MEMORY	3
	A. Physics of the Recording Process	3
	1. Electron Beam Heating Process	6
	2. Metallic Covered Target	15
	B. Memory System Consideration	19
	1. Maximum Beam Current	19
	2. Signal Detection Limitation	21
III	ELECTRON BEAM READOUT SENSITIVITY OF AMORPHOUS SEMICONDUCTOR THIN FILMS	27
IV	PARTICIPATING TECHNICAL PERSONNEL	35
	REFERENCES	36

INTENTIONALLY BLANK

LIST OF ILLUSTRATIONS

Figure		Page
1	The basic operation elements of the electron beam memory using amorphous semiconductor thin film as the storage target. I_p is the incident primary electron beam current, I_s is the secondary electron current and I_T is the target current. δ^0 is the secondary yield of the amorphous phase and δ^1 is that of the crystalline phase --	4
2	High density electron beam recording in amorphous semiconductor. Electron source: 4 kv, 100 na. 1000Å thick flash evaporated $Ge_{37}Te_{60}As_3$ on Mo coated Si substrate --	5
3	Schematic of the computer simulation model ----------	7
4	The thermal properties as function of temperature of amorphouse semiconductor used in the computer simulation program----------	7
5	The surface temperature distribution of thick amorphous semiconductor for various beam current: (a) Temperature at beam center vs time; (b) Temperature profile at 0.1 μs; (c) Same as 5b at 1.0 μs; (d) Same as 5b at 1.6 μs ----------	10
6	The surface temperature distribution of 3750Å amorphous semiconductor thin film memory target on 4000Å Mo coated Si wafer for various beam current: (a) Temperature at beam center vs time; (b) Temperature profile at t = 1.0 μs ----------	11
7	Same as Fig. 6 for 2750Å amorphous semiconductor thin film target: (a) Temperature at beam center vs time; (b) Temperature profile at t = 1.0 μs ----------	12
8	Same as Fig. 6 for 1750Å to 2050Å amorphous semiconductor thin film target. I_p = 0.2, 0.4, and 0.6 μA curves are for 1750Å, I_p = 1.0, 1.5, and 2.0 μA curves are for 2050Å: (a) Temperature at beam center vs time; (b) Temperature profile at t = 1.0 μs ----------	13
9	Computer simulated peak surface temperature vs time for various crystallization temperatures (3750Å thick amorphous semiconductor target.) The electron beam is 5 kv with 2μ diameter ----------	14

List of Illustrations (continued)

Figure		Page
10	SEM micrograph of 1.4μ wide recording on metal overcoat memory target (2900X). Electron source: 10 kv, 40 na	16
11	Video signal by target current readout with 10 kv electron. Base width of signal is about 1.4μ	17
12	Target readout modulation efficiency of the recording shown in Fig. 10	18
13	The physical constraints on the possible speed-density characteristics of amorphous semiconductor electron beam memory	20
14	Nomograph of possible I_p vs Δf and bit density for some dispenser cathode parameters. Target readout assumes a C_T = 25 pf	24
15	The upper limits of Δf vs beam diameter for J = 10 A/cm^2. The assumed parameters are listed in the figures. J = 100 A/cm^2 was assumed for the Schottky emission cathode	25
16	Schematic of the rotable sample stage apparatus for measuring δ vs angle	28
17	Photograph of the rotatable stage apparatus. The collector has been removed	29
18	Measured $\ln(\delta_0/\delta_0)$ vs $(1-\cos\theta)$ for amorphous form of $Ge_{37}Te_{60}As_3$. θ is the angle of incidence	30
19	Measured $\ln(\delta_0/\delta_0)$ vs $(1-\cos\theta)$ for Mo	31
20	The angular coefficient, k, for amorphous and crystalline forms of $Ge_{37}Te_{60}As_3$ vs beam voltage	32
21	The angular coefficient, k, for Mo vs beam voltage	33
22	Theoretical modulation efficiency vs angle of surface deformation for some values of k	34

I. INTRODUCTION

This is the first semiannual technical report on the research program, Interaction Between Amorphous Semiconductor Thin Film and Electron Beam, sponsored by the U.S. Army Research Office, Durham, North Carolina and the Advanced Research Projects Agency, Arlington, Va. under contract DAHC 04-72-C-0016. The report describes the research conducted during the period Feb. 7, 1972 to Aug. 6, 1972 as well as summarize the research conducted by the investigators on this subject prior to the above period.

The objective of the program is to gain an increased understanding of the switching properties of amorphous semiconductor thin films by the use of electron beam as a diagnostic tool. In addition amorphous semiconductor thin films appear to be an excellent candidate as a storage medium in an electron beam computer memory device. Because of the potential utility of amorphous semiconductor thin films in the above device, the research program has been enlarged to encompass a study of the possible device and system characteristics of an amorphous semiconductor electron beam memory.

We have done considerable work during the period when the proposed research was under the sponsors' evaluation. As this is the first technical report of the sponsored research program, a status summary of our research which includes our research prior to the contract period appears to be in order. Thus the first part of this technical report summarizes our present understanding of the interaction between amorphous semiconductor thin films and electron beam and the potential device and system characteristics of an amorphous semiconductor electron beam memory which exploits this interaction. Parts of this work was done prior to the contract period and parts of this work was completed during the contract period.

Based upon the fundamental physical limitations of device operation, we have developed a good qualitative understanding of the possible device and system characteristics of the amorphous semiconductor electron beam memory. To obtain quantitative understanding, we are now concentrating on the initial objective of this research program: an understanding of the interaction between amorphous semiconductors and electron beams.

The first phase of this investigation is to determine the possible readout sensitivity or the potential modulation efficiency of amorphous semiconductor thin films as an electron beam memory medium. Some aspect of this problem was examined in our reported work on the secondary yield in amorphous semiconductor thin films. We have continued this research and have derived theory of modulation efficiency for recording by surface deformation. The angular dependence of the secondary yield of amorphous semiconductor and Mo has been measured to determine quantitatively the possible modulation efficiency of this memory. This work constitutes the second part of this report.

The second phase is to understand the write sensitivity or the potential "speed" of amorphous semiconductor thin films as an electron beam recording medium. This work is in the preliminary stage and will not be covered in this report.

II. A SYSTEM CONSIDERATION OF AMORPHOUS SEMICONDUCTOR ELECTRON BEAM MEMORY

The increasing need for on-line mass storage with electronic access speed has been well documented.[1] With the development of the Fly's Eye electron optics,[2] electronic access to a large data base (10^9 to 10^{10} bits) on a stationary target in an electron beam mass memory appears to be feasible. A principal concern, however, has been the form of the memory storage target. To be economically and technologically viable, the memory target should fulfill the following requirements: same write and read beam voltage, high bit density without any physical defining structures, no external processing, and reasonable interaction energy with electron beam and suitable for high vacuum.

Thin films of chalcogenide glasses or amorphous semiconductors satisfy all these requirements and appear to be most suitable as read-mostly or as archival storage media.[3] The storage mechanism is the amorphous-to-crystalline phase transition and exhibits NDRO, nonvolatility, permanency, high density, and radiation resistance characteristics. The nature of the storage mechanism makes unlimited erasability unlikely. However, the need or even the desirability of erasability in such a mass storage has been questioned.[4, 5] For these reasons, we shall be primarily concerned with archival storage applications.

A. PHYSICS OF THE RECORDING PROCESS

The basic operational elements of such a memory are shown in Fig. 1. The amorphous semiconductor thin film storage target is structureless in that no physical entities such as metallic spots or holes are required to define the memory sites. Thus the bit position is defined by the electron beam, and its size is limited only by the beam diameter and the possible interaction between the thin film and the electron beam. Viewed simply, writing is accomplished by electron beam heating to induce the amorphous-to-crystalline transition. Readout by the electron beam is possible by the use of a lower beam current, at the same beam voltage, to measure the difference in secondary electron yields of the two phases. If we assume the amorphous phase to be the "0" state, then $I_s^0 = \delta^0 I_p$, where δ^0 is the yield of the amorphous phase. Similarly, δ^1 is the yield of the crystalline phase which is then the "1" state of the memory. As shown in Fig. 1, the secondary electrons can be measured either directly by an electron detector or indirectly by measuring the target current. The second method is possible as shown by the equation in Fig. 1.

An important concept in such a memory is that one need only to switch or to change the state of the surface of the film as secondary electrons are generated within a few hundred angstroms from the surface. Thus, it is

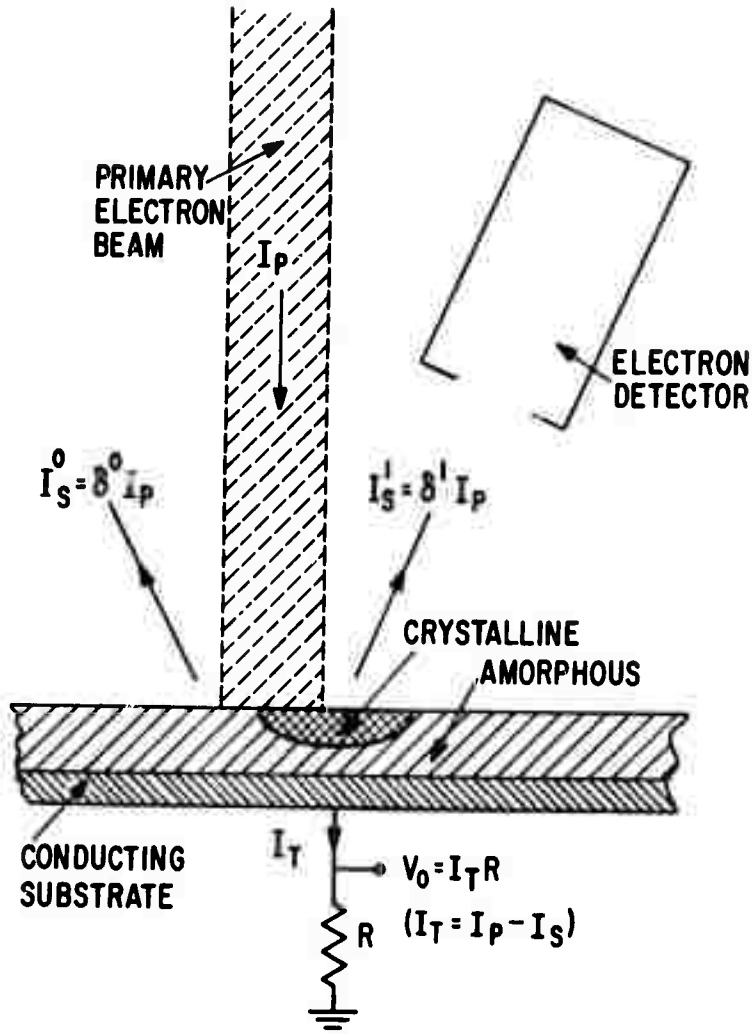

Figure 1 The basic operation elements of the electron beam memory using amorphous semiconductor thin film as the storage target. I_p is the incident primary electron beam current, I_s is the secondary electron current, and I_T is the target current. δ^0 is the secondary yield of the amorphous phase and δ^1 is that of the crystalline phase.

hoped that the electron beam heating duration can be short to obtain a memory spot size approximately equal to the beam diameter.

This simple picture of the operation of the memory will be modified if electron-beam enhanced crystallization, similar to photocrystallization, occurs during the write process.[6, 7] Fast ($\lesssim 10$ μsec) electron-beam induced memory switching observed in the chalcogenide thin films suggests that some form of enhanced crystallization process may occur.[3] Before any crystallization can occur, however, the amorphous semiconductor must be heated above T_g, the glass transition temperature. Nondestructure readout would

require that any beam heating which may occur during the read process be limited to below T_g.

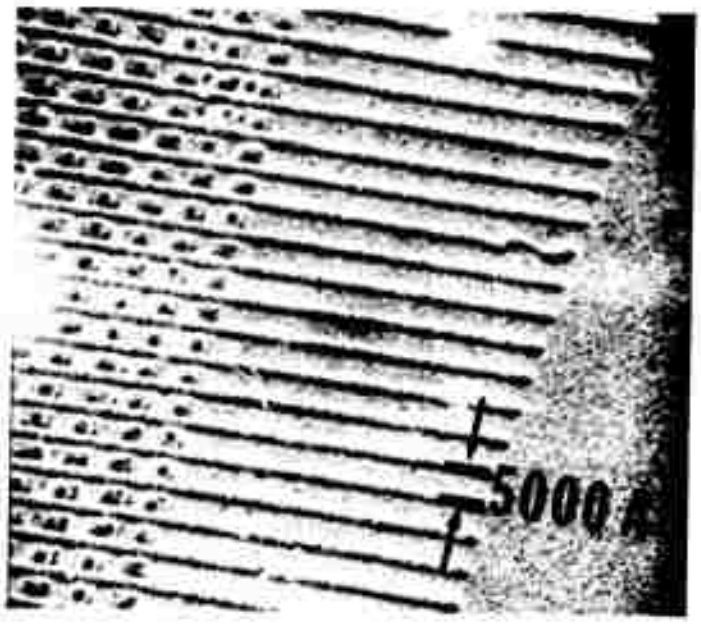

Figure 2 High density electron beam recording in amorphous semiconductor. Electron source: 4 kv, 100 na. 1000Å thick flash evaporated $Ge_{37}Te_{60}As_3$ on Mo-coated Si substrate.

An example of the electron beam recording capability of amorphous semiconductor thin film is shown in Fig. 2. The horizontal line recordings (~1000Å to 1500Å wide) were written with a high brightness thermionic field emission gun (4 kv, 100 na) at a scanning rate of 50 nsec per beam diameter (1000Å).[8] The good heat sinking substrate and the thin film thickness (1650Å) prevent any lateral heat spreading during the writing process. The film composition exhibited irreversible switching behavior; that is, the amorphous-to-crystalline phase transition was irreversible. In addition, the high thermal conductivity of the crystalline phase prevented the recording from being overwritten. Small dots between the horizontal lines rather than vertical lines resulted from an attempt to overwrite these horizontal lines. Besides high resolution, this example also shows that, with a sufficiently bright source, the rate of crystallization will not be an inhibiting factor in obtaining high memory writing speed in this medium. The high resolution, the high writing speed, and the stability of the recorded crystalline phase predicated the excellent quality of this medium for archival storage.

1. Electron Beam Heating Process

A good understanding of the electron beam heating and cooling processes is necessary to realize such a memory. Among the important characteristics are: the minimum beam energy required to induce the crystallization during this process, and the design of thermal characteristics of the target to prevent heat spread beyond the beam diameter. These problems must be examined with time duration in the microsecond region and spatial variation of micron and submicron dimensions. Furthermore, the changes in the thermal parameters as the materials undergo these phase transitions must be considered.

Experimental determination of the details of the heating and cooling processes within the above time and spatial constraints appear to be extremely difficult, if not impossible. Analytical investigation of similar electron beam heating problems have been made by various workers.[9-11] Most of these treatments, however, were restricted to idealized geometrical situations, and none of them treated the problem with temperature dependent thermal parameters. Computer simulation offers an attractive and perhaps the only alternative solution to this problem. The simulation of the heating and cooling processes in an amorphous semiconductor beam memory has been carried out using the THTD program.

The geometry considered in the computer simulation model is shown in Fig. 3. It is a layer-structure model in which a thin film of amorphous semiconductor is deposited upon a molybdenum-coated silicon substrate. The electron beam is assumed to have uniform current density with finite radius and to dissipate its energy within the amorphous semiconductor to the depth of the electron penetration range.

For the particular geometry shown in Fig. 3, the volume was partitioned into 260 segments of various sizes. Fine segment sizes were used at the boundaries of the volume heated by the electron beam to account for the expected large thermal gradient. All external surfaces had adiabatic boundary conditions. To simulate the large size of the memory target accurately, the temperature of the peripheral segments cannot change from its initial value (room temperature) for any valid solution.

For our particular problem, the electron is assumed to dissipate all its energy into heat uniformally within the volume defined by its diameter and the penetration range of the electron. The penetration range used is based on the empirical relationship given by Kobetich and Katz.[12]

A particularly troublesome problem in our simulation are the values of the thermal properties of the target materials. In general, we have used the values for silicon and molybdenum tabulated by the TPRC Data Series.[13] For the amorphous semiconductor which will undergo amorphous-to-crystalline and crystalline-to-liquid phase transitions, we have used the thermal conductivity and specific heat shown in Fig. 4. As we are concerned with tellurium-

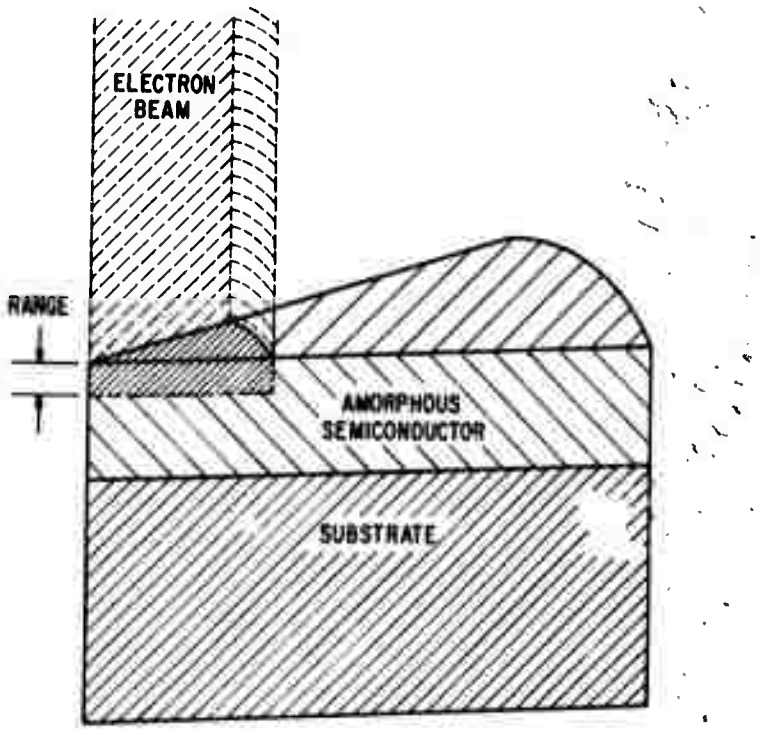

Figure 3 Schematic of the computer simulation model.

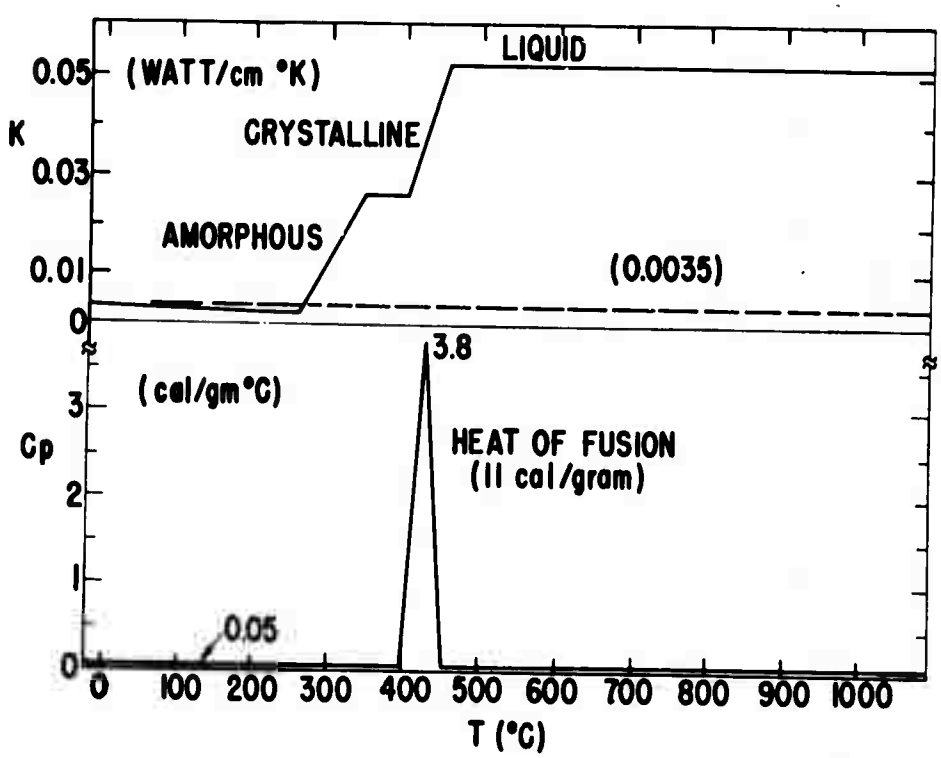

Figure 4 The thermal properties as function of temperature of amorphous semiconductor used in the computer simulation program.

based chalcogenide glasses, the crystalline and liquid thermal conductivity and specific heat shown in Fig. 4 are those of Te given in the TPRC Data Series.[13] The value of thermal conductivity, K, in the amorphous phase is one-tenth that of crystalline Te. This extrapolation is based on the similar ratio measured for Se,[13] and is close to the value of the commercial Ge-Sb-Se infrared glasses.[14]

The melting point, 425°C, is near that of the Ge-Te eutectic. As we are concerned with the minimum or the worse case electron beam energy necessary to crystallize the amorphous semiconductor thin film at heating rates (>100°C/μsec) much faster than the normal DTA measurement rates, we have arbitrarily chosen a high crystallization temperature of ~315°C. Crystallization is assumed to occur immediately at this temperature because of its rate will be enhanced by the electron beam excitation. The crystallization process was assumed to occur over a span of 50°C. To simulate the heat of fusion upon melting, the specific heat has a large "spike" at the melting point. The base width was 50°C wide and the peak value was based on a heat of fusion of 11 cal/g. This value is close to the measured heat of crystallization of Ge-Te-As glasses[15] but may be too small by a factor of two. The inclusion of this large heat of fusion, however, is needed and does provide a realistic simulation of the effect of heat of fusion on the heating and cooling processes.

By our choice of the thermal boundary conditions, we have neglected the possible heat loss caused by radiation. Even though the emissivity from these materials may be high,[16] this loss will be orders of magnitude less than the conduction losses for the temperature region (<1000°K) under consideration.

Perhaps a more serious problem is that we have not included the possible effects of the heat of crystallization in our simulation. In part, this is due to our ignorance on the rate of this heat release and in part on the difficulty in incorporating this effect in our simulation program in concert with the time transient response. Physically, the effect of any heat released upon crystallization will increase our simulated heating rate and perhaps the peak temperature. The magnitude of this effect will depend in part on the time duration of this heat release. For these reasons, our results of the surface temperature will be the minimum attainable for the given electron beam excitation.

The electron beam parameters were chosen to reflect the state-of-the-art of conventional electron gun sources and the desirable data rate of a potential memory. Thus the electron beam was assumed to be at 5 kv with a diameter of 2μ. The pulse duration was 1 μsec with less than 10 nsec rise and fall time. Thus the heating and cooling processes needed to achieve a data rate of greater than 1 MHz can be studied. The maximum beam current studied was 1 μA and reflects the present state-of-the-art for conventional long life, high brightness electron guns.[17] The penetration range of the 5 kv electron used is 1750Å and is based on a thin film density of ~5 g/cm^3. Instead of varying the beam parameters, it is more instructive to examine the thermal behavior of the various amorphous semiconductor targets for the above electron beam source.

Because the memory depends primarily on the change induced on the surface of the amorphous semiconductor thin film, the temperature of the surface (~250Å deep) as a function of time and as a function of radial distance will be our primary concern.

The temperature profiles were determined for various targets to evaluate the necessary beam power for writing and the maximum permissible beam current for reading. As a reference, the surface temperature vs time and the temperature profiles for various beam current for the thick (80μ) amorphous semiconductor target were evaluated. The results are shown in Figs. 5(a) through (d). As one can see, a beam current of 0.2 μA is sufficient to heat the material to the crystallization temperature, and at the same time no surface is heated to the melting point. The reading current, however, will have to be less than 0.1 μA if we assume $T_g < 200°C$.

The temperature profiles at three time frames are shown in Figs. 5(b), (c), and (d). As expected, at 0.6 μsec after the beam cutoff (t = 1.6 μsec) the temperature has a diffusion-like profile modified, of course, by the effects of the phase transitions. Although low beam currents can be used to write, the long cooling time of the surface temperature from above the melting point is a serious handicap for fast data rate.

The temperature distributions for 3750Å, 2750Å, and 1750Å to 2050Å thick films are shown in Figs. 6(a) through 8(b). As expected, the beam current required to write has increased with decreasing film thickness and the cooling decay time has decreased considerably (<0.5 μsec) from that of the thick, amorphous semiconductor. An additional benefits of the heat sinking substrate is that the heat spread beyond the beam edge is also smaller.

The peak in the temperature vs time curve observed for certain beam currents [i.e., 1.0 μA in Fig. 6(a)] occurs at the time when the temperature at the beam edge crosses the melting point. Physically we can postulate that, at that time, the material adjacent to the beam increased its thermal conductivity and under this condition the beam power is insufficient to support the high peak temperature. Whether this temperature peak will actually develop in a real-life situation is an open question.

The loss in heating efficiency as measured by the difference in the peak temperature of 3750Å film in comparison to the thick film is very small. This loss appears to be a weak function of the film thickness until a certain minimum threshold level is reached. At 2050Å, even a beam current of 1.0 μA is insufficient to heat the 2μ diameter surface to the melting point. Qualitatively speaking, at 5 kv, a film thickness of twice the penetration range of the electrons appears to be an optimum choice in the balance between the high beam heating efficiency and the fast cooling thermal time constant desired.

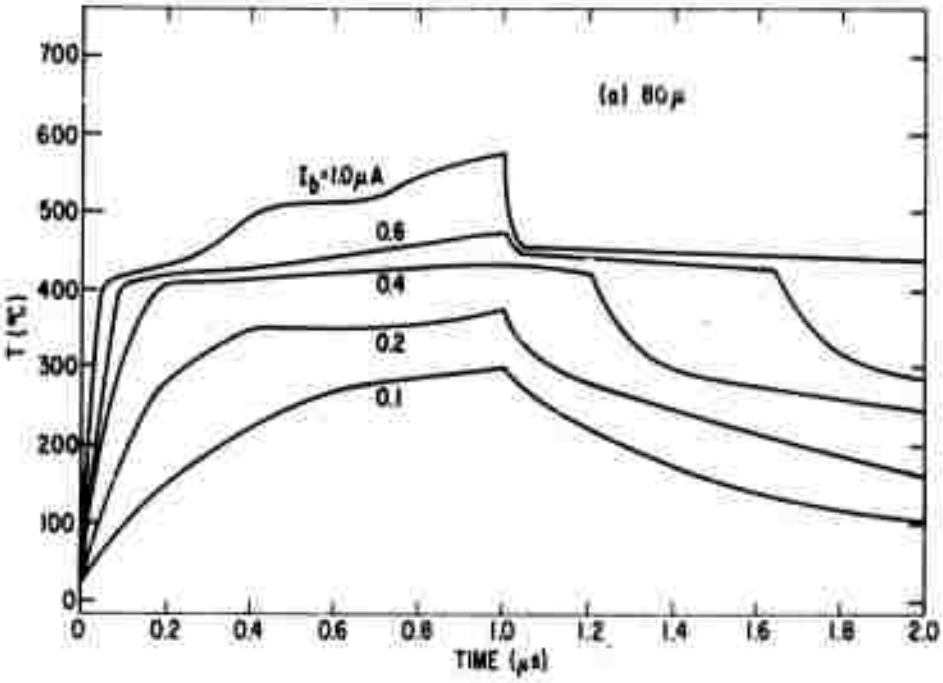

(a) Temperature at beam center vs time.

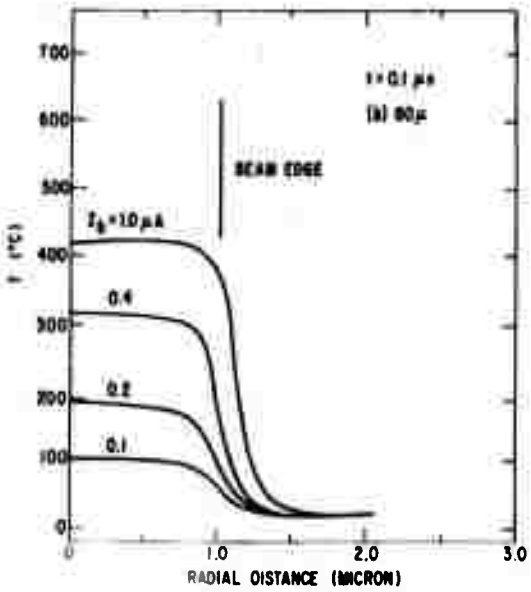

(b) Temperature profile at 0.1 μsec.

Figure 5 The surface temperature distribution of thick amorphous semiconductor for various beam currents.

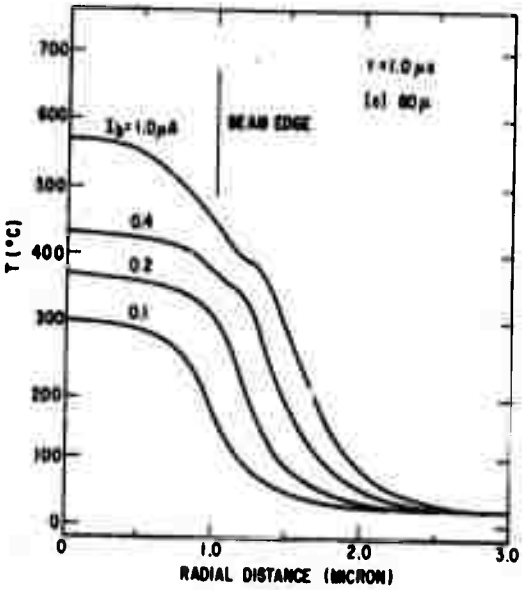

(c) Same as 5(b) at 1.0 μsec.

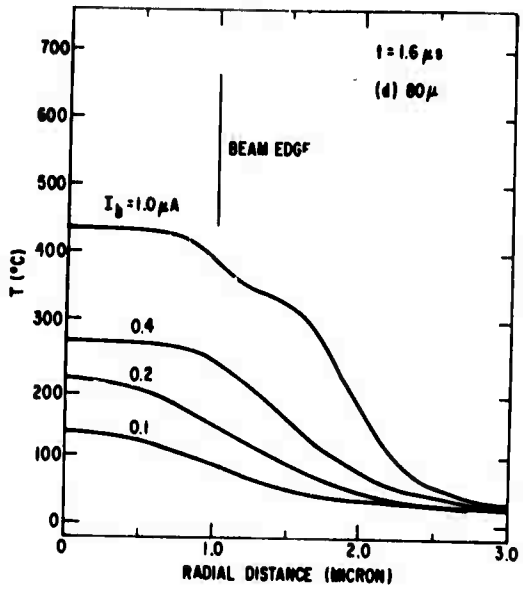

(d) Same as 5(b) at 1.6 μsec.

Figure 5 (concluded)

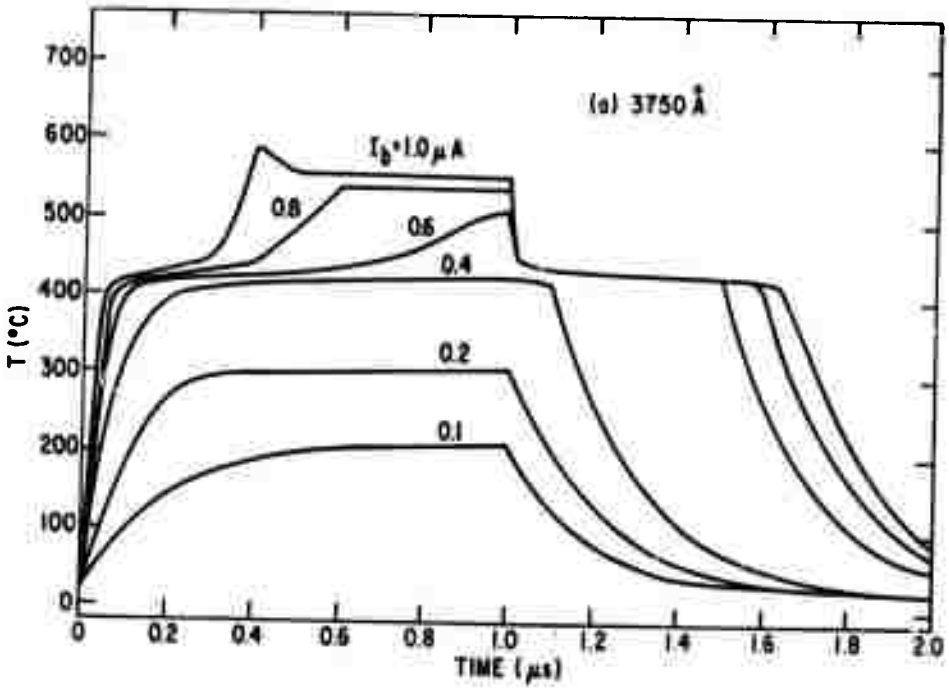

(a) Temperature at beam center vs time.

Figure 6 The surface temperature distribution of 3750Å amorphous semiconductor thin film memory target on 4000Å Mo-coated Si wafer for various beam current.

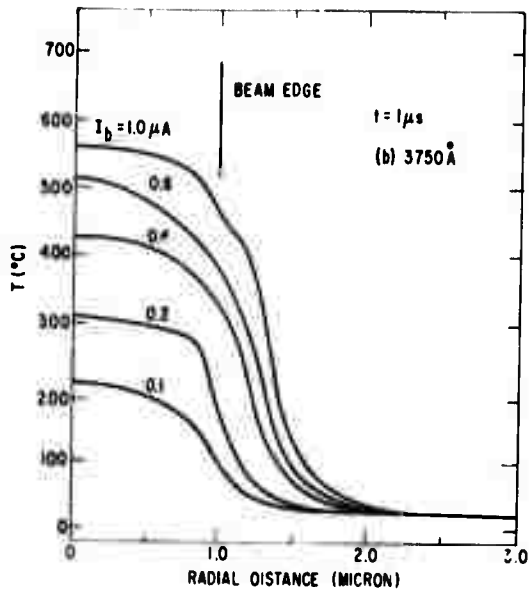

(b) Temperature profile at
t = 1.0 μsec.

Figure 6 (concluded)

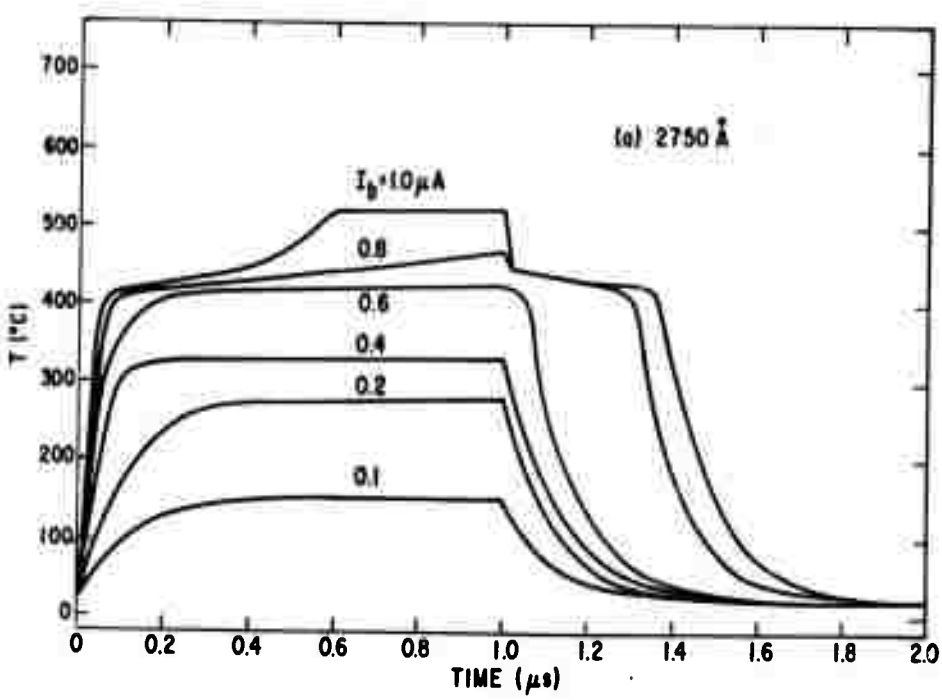

(a) Temperature at beam center vs time.

Figure 7 Same as Fig. 6 for 2750Å amorphous semiconductor thin film target.

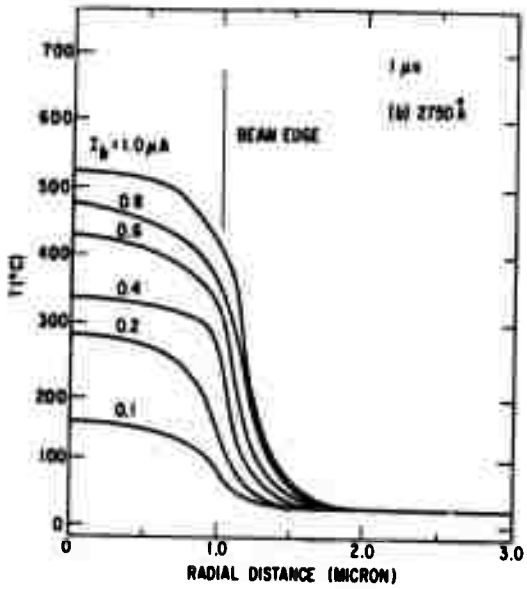

(b) Temperature profile at
t = 1.0 μsec.

Figure 7 (concluded)

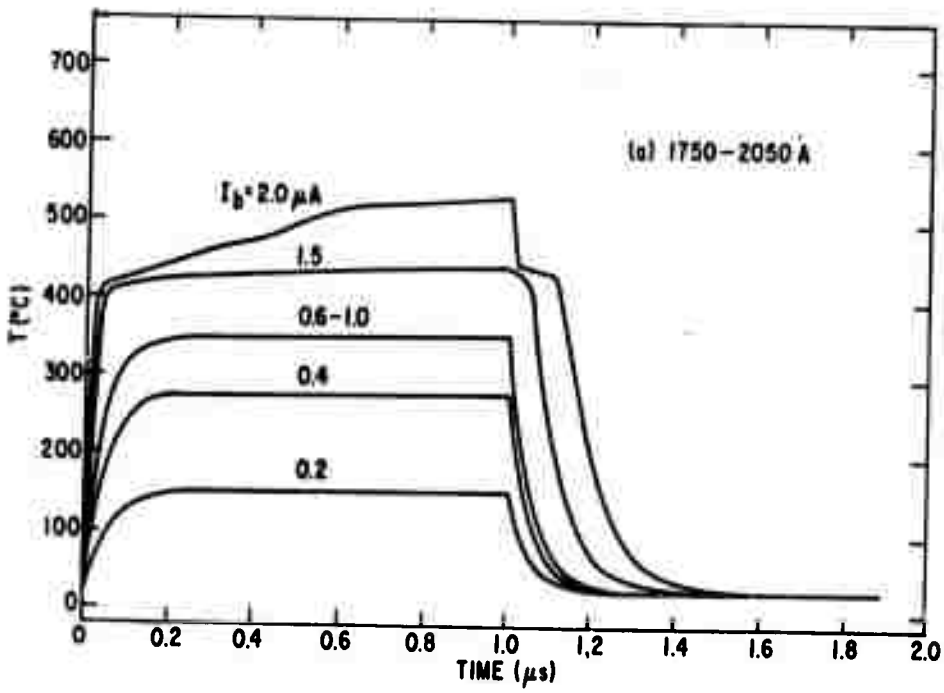

(a) Temperature at beam center vs time.

Figure 8 Same as Fig. 6 for 1750Å to 2050Å amorphous semiconductor thin film target. I_p = 0.2, 0.4, and 0.6 μA curves are for 1750Å; I_p = 1.0, 1.5, and 2.0 μA curves are for 2050Å.

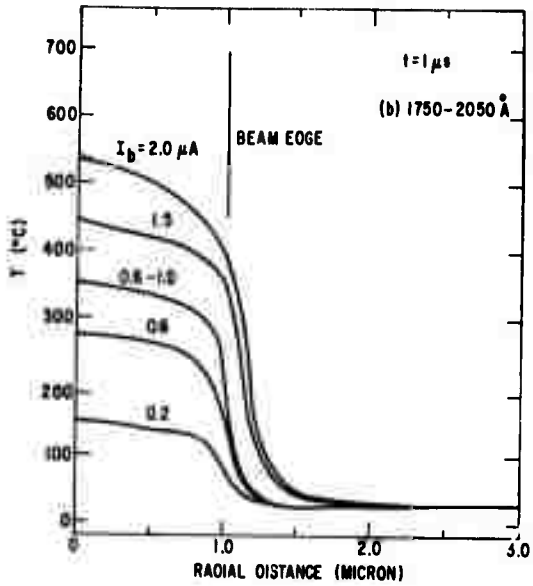

(b) Temperature profile at
t = 1.0 μsec.

Figure 8 (concluded)

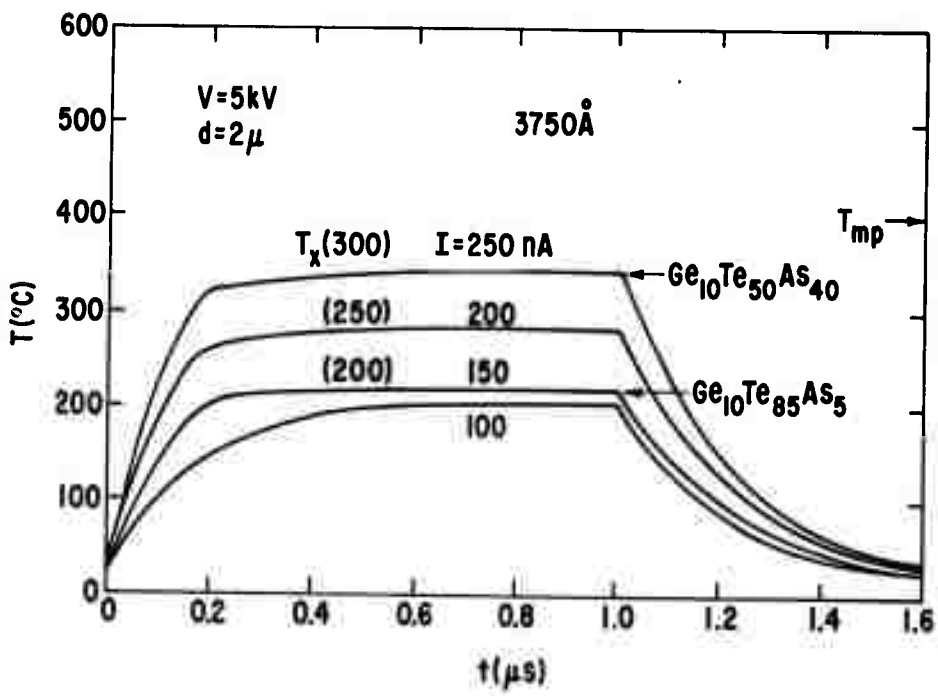

Figure 9 Computer simulated peak surface temperature vs time for various crystallization temperatures (3750Å thick amorphous semiconductor target.) The electron beam is 5 kv with 2μ diameter.

The maximum reading beam current depends on the glass transition temperature. If this temperature is 150°C, then 0.1 μA is too high for 3750Å but permissible for 2750Å film target.

The effect of the change in crystallization temperature, T_x, on the required beam current to write has also been evaluated. Figure 9 shows the change in writing beam current when T_x is altered between 200° and 300°C by varying the Te content of the Ge-Te-As thin film.

2. Metallic Covered Target

The electron beam readout operation of amorphous semiconductor thin film has been described primarily in terms of change of secondary yield between the amorphous and the crystalline phases. However, there appear to be two potentially disadvantages with this method. One is that the change in secondary yield is a material parameter for which no theoretical base has yet been established. Thus this change must be empirically measured for each particular chalcogenide composition. In addition, the change in secondary yield may be small for certain compositions which may be highly desirable storage targets because of other memory system considerations. For example, an irreversible composition is highly desirable for archival memory applications. Yet the change in yield for a particular irreversible composition was measured to be only 10% for incident beam voltage of 1 to 5 kv.[18] Furthermore, there is some concern on the possible effect of potential surface contamination on the stability of this change in secondary yield.

Readout by surface deformation is an alternate mode which may alleviate some of the difficulties cited above. In this mode the change in secondary yield is due to the oblique incidence of the primary beam on the surface deformed by the amorphous-to-crystalline transition. The readout modulation efficiency may be made insensitive to the secondary yield of the amorphous semiconductor by covering the target with a thin (~100Å) metallic film.

Preliminary verification of this recording technique was carried out with a 5000Å film of $Ge_6Te_{66}As_{26}$ covered by 100Å of Mo. An SEM was used as the electron beam source. Figure 10 shows the three vertical recordings made by a line scanning 10 kv electron beam. The beam diameter was about 1.0μ and the writing beam current was 40 na. The three lines were written with 10, 20, and 50 msec dwell time per beam diameter. The similarities of these recordings show that as predicated by computer simulation the writing process has a wide margin. The serpentine patterns were the result of the slow beam heating process. They do not occur at higher writing speeds and their origin is not understood. If we assume the crystallization temperature to be about 200°C,[20] then the writing beam current is approximately the same as the computer simulation results. Some video signals of various cross sections of these 1.4μ wide recordings from target current readout at 10 kv are shown in Fig. 11. The enhanced signal at the edge of the deformation is very evident.

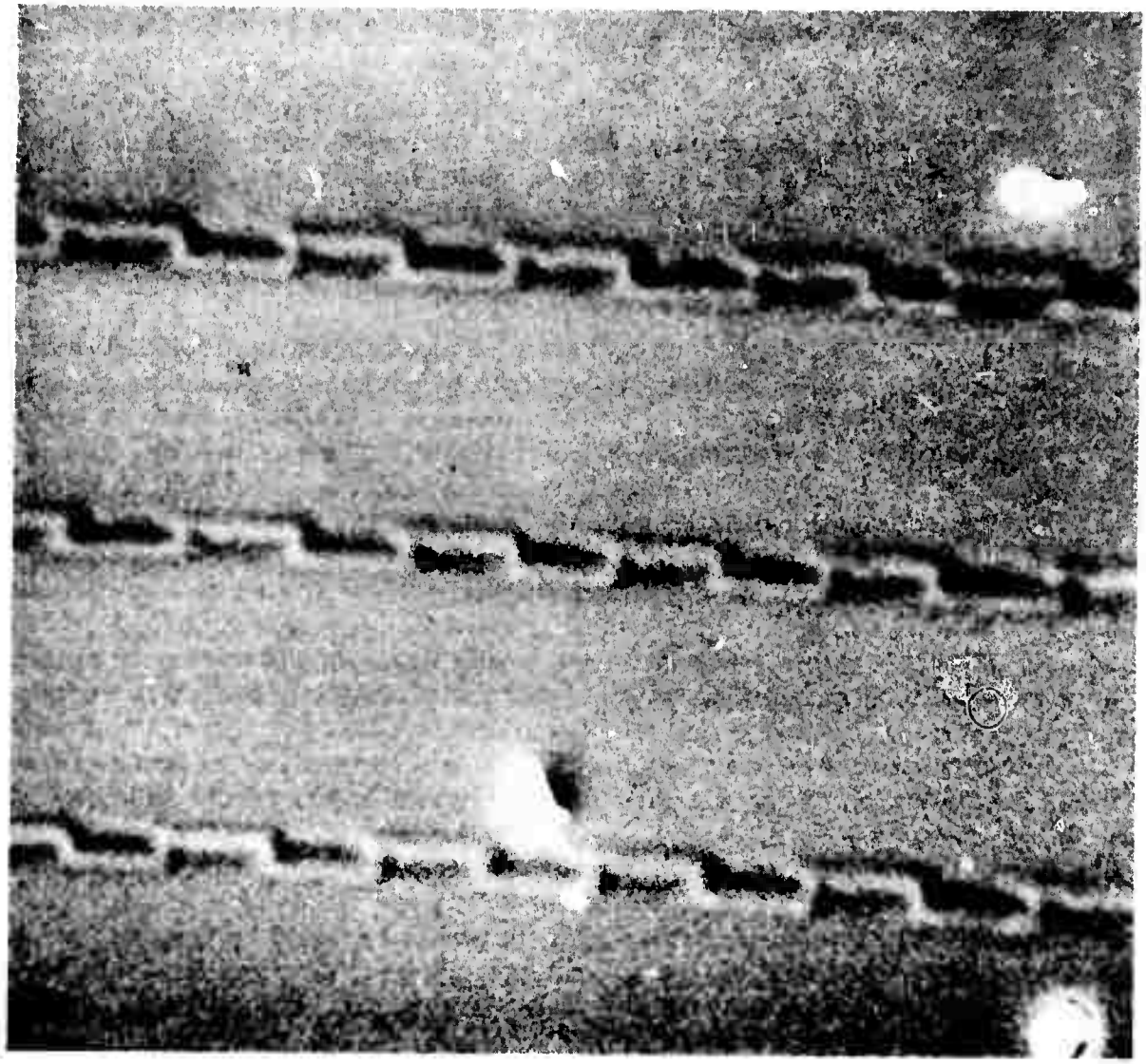

Figure 10 SEM micrograph of 1.4μ wide recording on metal overcoat memory target (2494X). Electron source: 10 kv, 40 na.

A qualitative measure of the modulation efficiency of this readout process was determined by comparing the video signals with and without the beam current. The results are shown in Fig. 12. The efficiencies increased with decreased beam voltages--14% at 10 kv, 16.7% at 5 kv, and 43% at 3 kv. However, the reasons for this change are not understood and are presently being investigated.

Although these results are qualitative as the secondary electron collection efficiency may differ between an SEM and a specially designed electron beam memory, they do hold the promise that high modulation efficiencies are possible with this recording technique.

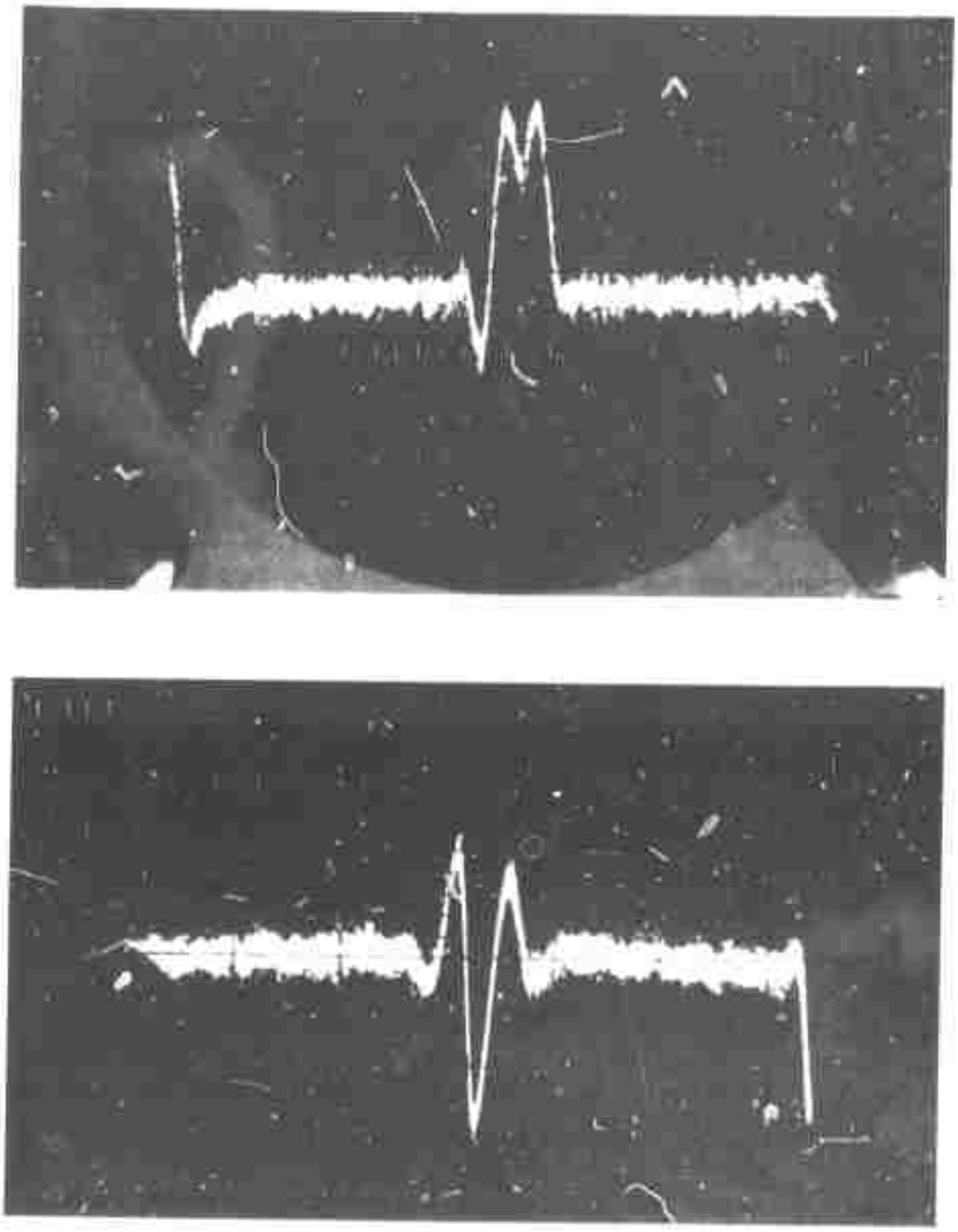

Figure 11 Video signal by target current readout with 10 kv electrons. Base width of signal is about 1.4μ.

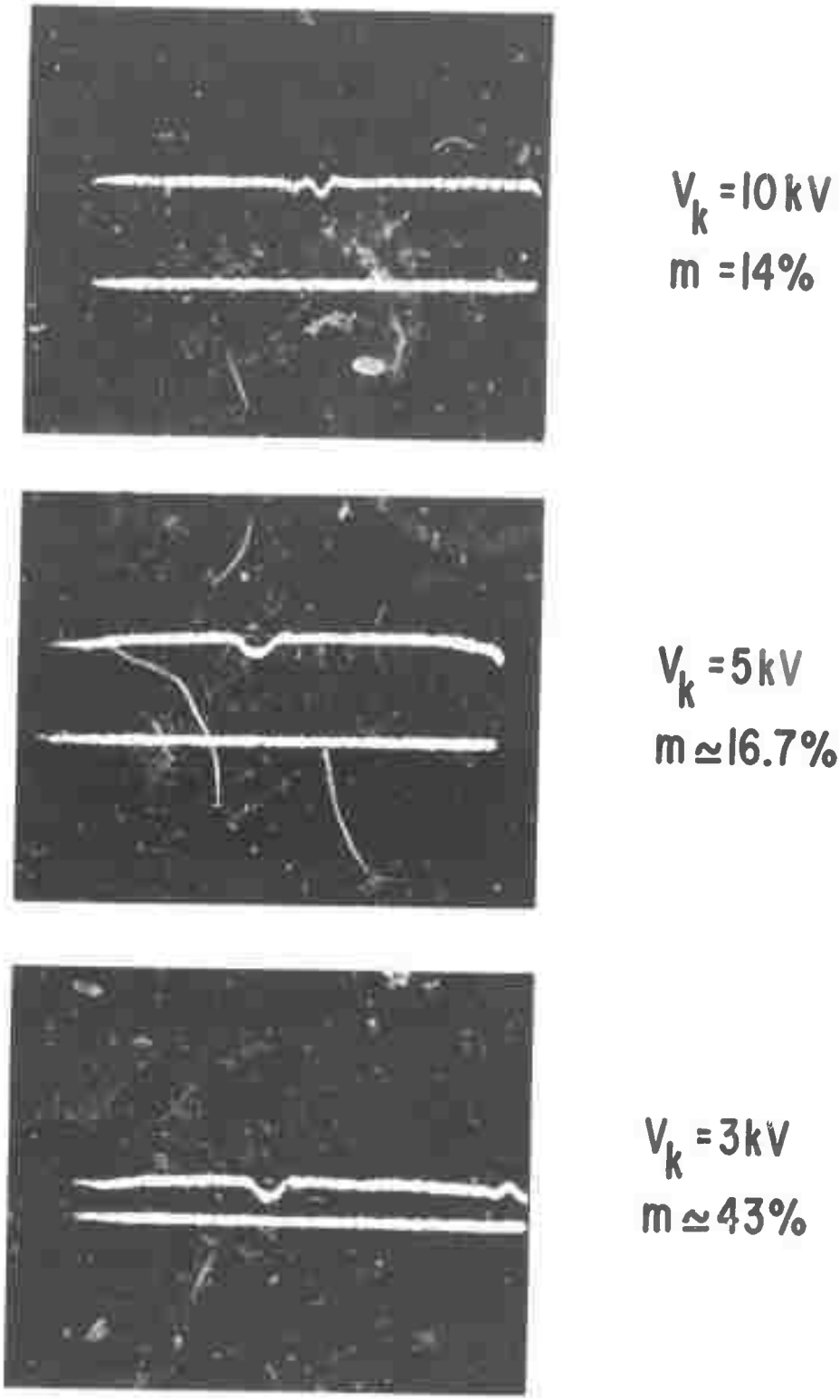

Figure 12 Target readout modulation efficiency of the recording shown in Fig. 10.

B. MEMORY SYSTEM CONSIDERATIONS

Any electron beam memory system requires the consideration of the electron source, electron optics and its control, memory target, and data recovery. However, without a detailed design, one can derive certain fundamental speed-density limitations for this form of beam memory. This relationship takes account of the following factors:

1. Limited beam current density--The physical laws of optics limits the possible beam current density one can obtain from a source of given brightness.

2. Signal detection limitations--Any readout mechanism would be limited by the shot noise from the beam as well as possible Johnson's noise from the target current measuring resistor.

3. Error rate--The acceptable error rate determines the minimum signal-to-noise (S/N) ratio requirements which in turn determine the maximum frequency of operation. We have required a signal-to-noise ratio of greater than 10.0, which implies an approximate error rate of about one in 10^{-7}.[21]

These factors which constrain the performance characteristics of the memory are shown in Fig. 13.

1. Maximum Beam Current

The limited beam current at the target can be derived based upon Langmuir's limit.[22] The maximum beam current, I_p, is

$$I_p \simeq \frac{\pi}{4} d_0^2 j_0 \left(\frac{eV}{kT}\right) \alpha^2 \tag{1}$$

where j_0 is the cathode current density, d_0 is the beam diameter for aberrationless electron optics, V is beam landing potential, and α is the half-angle of the converging beam at the target. Equation (1) assumes that $eV/kT >> 1$ and $\alpha << 1$ are the operating conditions.

If we assume Gaussian optics and that spherical aberration is the dominant imperfection in the electron optics, we have for the actual beam diameter, d,

$$d^2 = d_0^2 + \left(\frac{C_s}{2}\right)^2 \alpha^6 \tag{2}$$

where C_s is the spherical aberration coefficient. For the anticipated operation of a beam memory with low beam current and kv electrons, the

MEMORY SYSTEM CONSTRAINTS

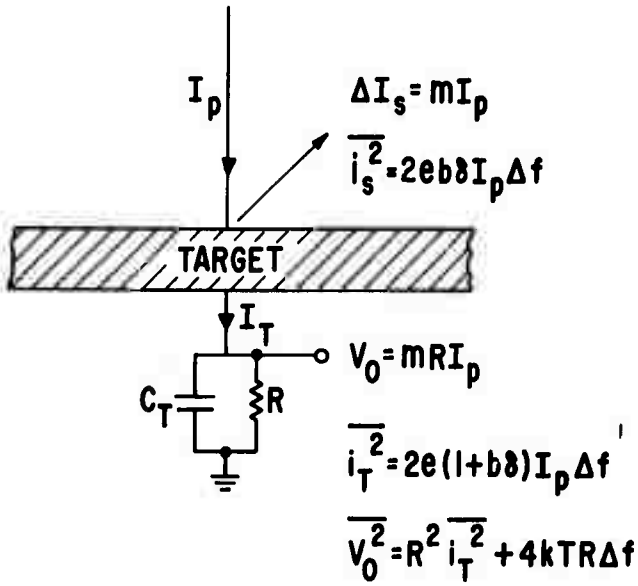

- LIMITED BEAM CURRENT DENSITY
- SHOT NOISE OF THE BEAM
- JOHNSON NOISE
- ERROR RATE (S/N RATIO)

Figure 13 The physical constraints on the possible speed-density characteristics of amorphous semiconductor electron beam memory.

assumptions made for Eqs. (1) and (2) are reasonable. Substitute Eq. (2) into (1) and find the maximum beam current with respect to α; i.e., solve $\partial I_p/\partial\alpha = 0$, we find that

$$I_p\Big)_{max} = \frac{3\pi}{16}\, j_0 \left(\frac{eV}{kT}\right) d^2\, \alpha^2_{max} \tag{3}$$

where

$$\alpha^3_{max} = \left(\frac{d}{C_s}\right) . \tag{4}$$

Equation (3), which gives the maximum beam current for an electron optics of a given C_s, is within 20% of the theoretical limited derived by Hughes[23] if d encompasses 90% of the total beam current. Equation (3) does not take

into account of any loss in efficiency due to losses in the electron gun or in the real electron optics. However, this maximum limitation on the beam current is elieved to be a good realistic estimate as electron source brightness of more than 80% of the theoretical limit has been reported.[17]

2. Signal Detection Limitation

To determine the fundamental limitation in signal detection we have considered only the basic noise contributions of the readout process-shot noise of the beam and Johnson's noise of any target resistor. Because of the high gain of most electron multipliers, amplifier contribution to the noise of secondary electron detection is small. Similarly, because of the small beam current ($<10^{-7}$ amp) of the memory, the target resistor will have to be large. Thus Johnson's noise will be the predominant noise in target readout.

In addition, because writing is a thermal process it will inevitably be slower than the possible reading speed which will determine the speed-density limitation of the memory. In considering the maximum reading speed we have used the maximum beam current derived in the last section, and have neglected possible thermal limitation of the target.

For secondary electron detection, the readout noise is due to shot noise of the primary beam as well as the possible fluctuation in the secondary yield. This noise is similar to that experienced in a vacuum tube and is given by:[24]

$$\overline{i_s^2} = 2\, eb\delta I_p \Delta f. \tag{5}$$

b expresses the possible fluctuation in the secondary yield of the target; I_p is the primary current, and Δf is the bandwidth.

The modulated secondary electron output signal is

$$\Delta I_s = \frac{(\delta_{AMOR} - \delta_{CRYST})}{\delta} I_p \tag{6}$$

for the simple amorphous semiconductor target, or

$$\Delta I_s = \frac{(\Delta_\theta - \delta_0)}{\delta_0} I_p \tag{7}$$

for the metallic covered target. In either case we can define the modulation coefficient, m, by

$$\Delta I_s = mI_p . \tag{8}$$

Using Eqs. (5) and (8), the signal-to-noise ratio is

$$\frac{S}{N} = \frac{mI_p}{(\overline{i_s^2})^{1/2}} \tag{9A}$$

$$= \frac{mI_p}{(2eb\delta I_p \Delta f)^{1/2}} \ . \tag{9B}$$

For a given S/N ratio as determined by minimum error rate, Eq. (9B) results in a limit on the beam current,

$$I_p > \frac{1}{m^2} \left(\frac{S}{N}\right)^2 \ 2eb\delta\Delta f \ . \tag{10}$$

For target readout we have for the target current, I_T,

$$I_T = I_p - I_s \ . \tag{11}$$

Thus if we assume that I_p and I_s are uncorrelated, the shot noise in I_T would be

$$\overline{i_T^2} = \overline{i_p^2} + \overline{i_s^2} \tag{12A}$$

$$= 2e\,(1 + b\delta)\ I_p \Delta f \ . \tag{12B}$$

It is bigger than $\overline{i_s^2}$ by the shot noise of the primary current.

In addition to the shot noise, the target current readout will have Johnson's noise contribution from the target resistor. Thus, the total target noise is

$$\overline{i_T^2} = 2e\,(1 + b\delta)\ I_p \Delta f + 4kT\Delta f/R \ . \tag{13}$$

As Johnson's noise is much larger than the shot noise, we have used

$$\overline{V_T^2} = R^2\,\overline{i_T^2} = 4kTR\Delta f \tag{14}$$

as the noise voltage for target current readout.

Similar to Eq. (8), we can define a target output signal by

$$V_T = mRI_p \tag{15}$$

where again m is the modulation coefficient. Thus the signal-to-noise ratio is:

$$\frac{S}{N} = \frac{mRI_p}{(4kTR\Delta f)^{1/2}} \quad . \tag{16}$$

However, in this case we can assume that for digital readout, R and the target capacitance, C_T, are related by the following constraint,

$$R < \frac{1}{2\pi C_T \Delta f}. \tag{17}$$

By inserting Eq. (17) into (16), we have for a given S/N ratio that the beam current must be greater by:

$$I_p > \frac{1}{m}\left(\frac{S}{N}\right)(8\pi kTC_T)^{1/2}\ \Delta f\ . \tag{18}$$

The above considerations have shown that once the required S/N ratio and signal bandwidth have been defined, the beam currents must exceed the criteria as given by Eqs. (10) and (18) for secondary electron and target readout, respectively. The maximum beam current available is constrained by Eq. (3).

In any recording process, the possible data rate is intimately related to the bandwidth. However, this relationship does depend on the recording format. For example, the data rate can be $2\Delta f$ for NRZ recording. For electron beam memory, one will probably use a form of biphase recording in which an information bit will be represented by two memory sites. Here again, to the first approximation the data rate can be $2\Delta f$; but the bit density has been decreased by 1/2. In addition, coding redundancies will also affect the effective information bit density. For the above reasons, the performance limitations of the amorphous semiconductor electron beam memory have been evaluated using Δf and d, the beam diameter, as parameters. In some cases we have used memory site density as a parameter where the density assumes a 50% guard band around each site.

A nomograph which gives this performance limitation in amorphous semiconductor memory for some electron beam sources is shown in Fig. 14. Two curves, I_p vs Δf and I_p vs density, are plotted on the same graph to determine the performance limitation. For example, at spot size of 0.5μ or a bit density of 1.5×10^9 bit/in^2, the maximum beam current would be 5×10^{-8} amp for $J_0 = 3$ A/cm^2 landing at 5 kv. Even with m = 1.0, target readout can be no more than 3 MHz assuming C_T = 25 pf. For secondary electron readout, m = 0.2 would be sufficient to obtain 20 MHz bandwidth.

An example of this performance limitation for a high brightness electron source (J_0 = 10 A/cm^2) is shown in Fig. 15. We see that Δf is strongly dependent on the beam diameter, i.e., $\Delta f \sim (d)^{8/3}$. Physically, it reflects the situation in which, as the beam diameter becomes smaller, the beam current also becomes smaller. And thus the frequency of operation must necessarily be decreased to provide the needed signal-to-noise ratio to maintain an acceptable error rate for practical memory operation.

The assumed electron source in this figure is an optimistic but attainable cathode loading for present-day, long-life conventional sources. The Schottky emission pointed cathode, which is a thermally aided field emission gun, has been described and used by many workers in electron microscopy.[25]

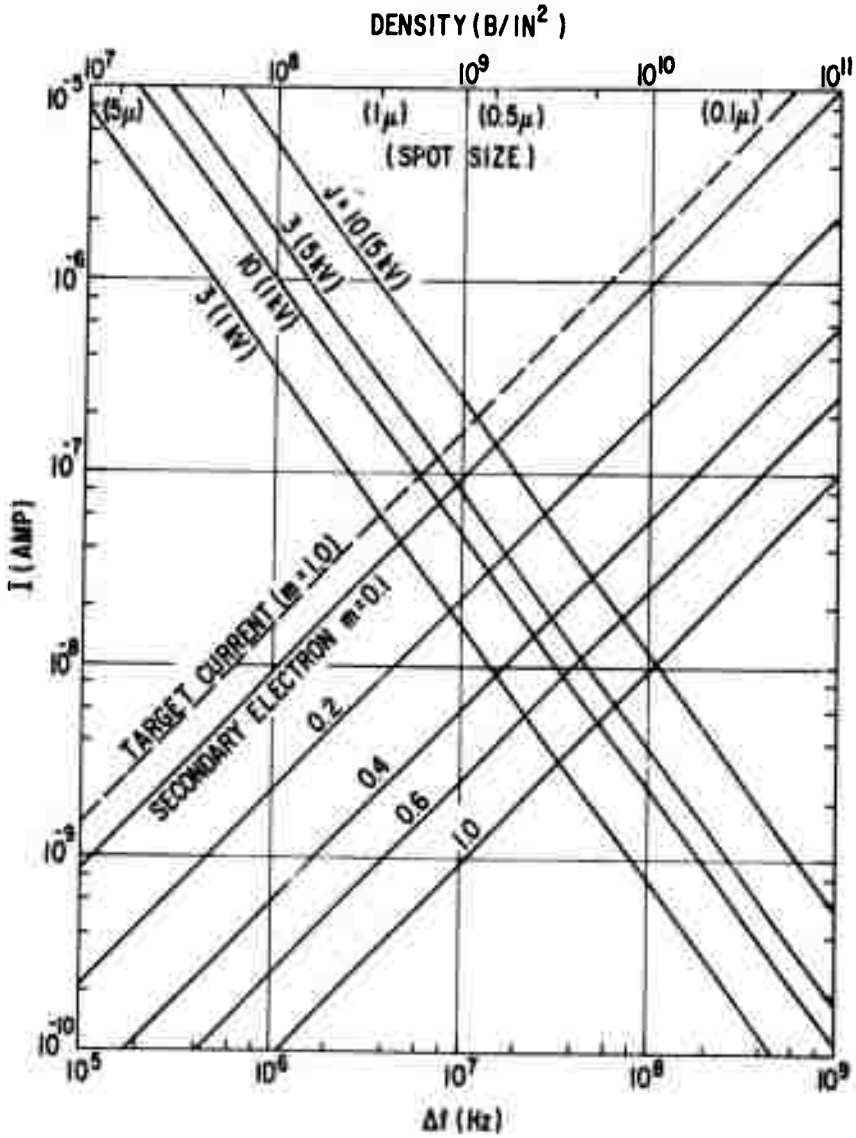

Figure 14 Nomograph of possible I_p vs Δf and bit density for some dispenser cathode parameters. Target readout assumes a C_T = 25 pf.

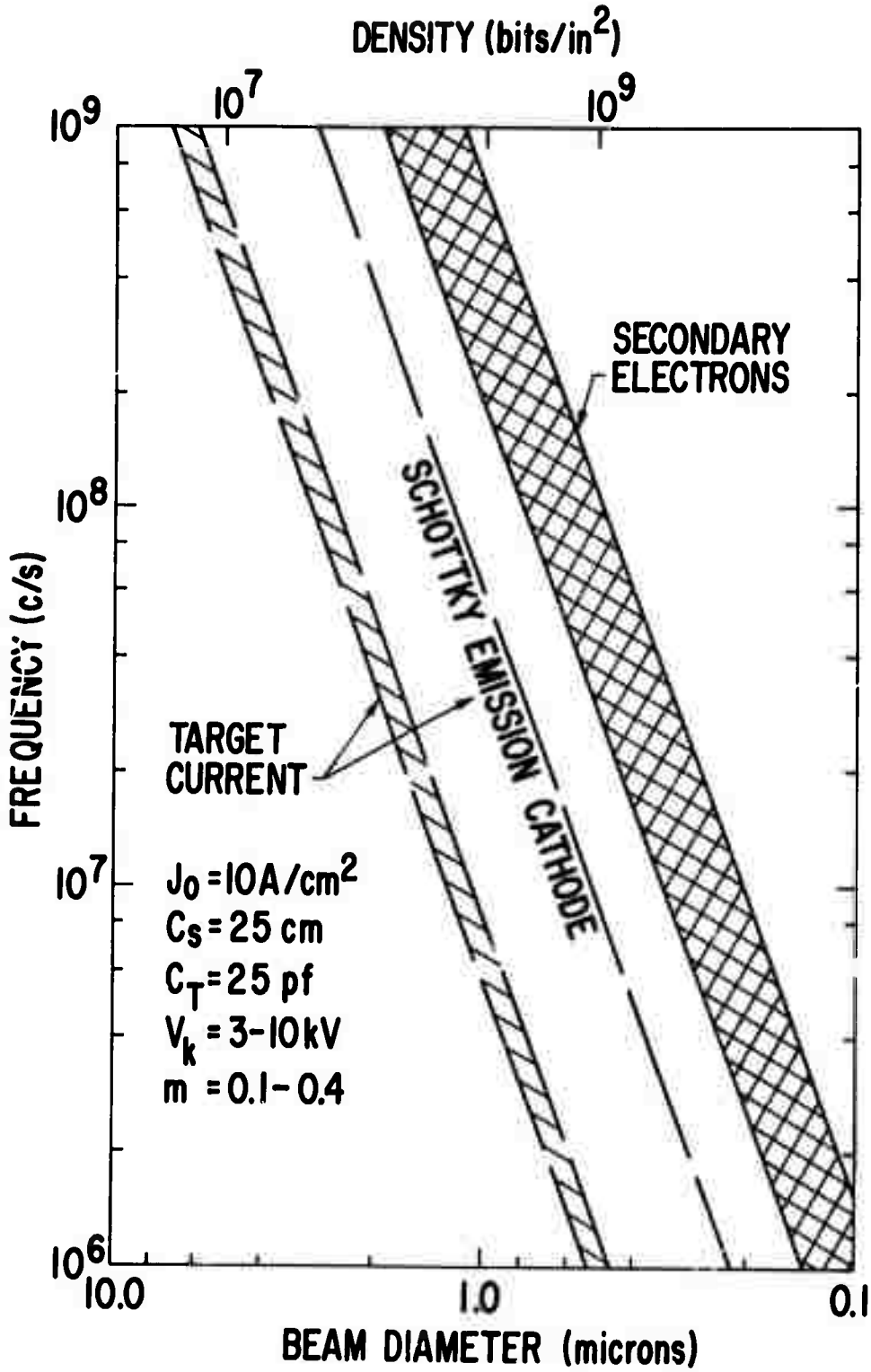

Figure 15 The upper limits of Δf vs beam diameter for $J = 10\ A/cm^2$. The assumed parameters are listed in the figures. $J = 100\ A/cm^2$ was assumed for the Schottky emission cathode.

TABLE I

Typical Speed-Density Limiting Values for Various Sources

	CATHODE LOADING					
	$3A/cm^2$		$10A/cm^2$		$100A/cm^2$	
BIT SIZE (μ)	0.5	1.0	0.5	1.0	0.5	1.0
DENSITY (b/in^2)	10^9	2.5×10^8	10^9	2.5×10^8	10^9	2.5×10^8
DATA RATE (MC/S)						
TGT READOUT	0.2	1.0	1.0	7.0	10.0	60.0
SEC. ELECTRONS	10.0	80.0	50.0	300.0		

ASSUMING: $C_S = 25$ cm $\quad V_k = 3\text{-}10$ kV
$C_T = 25$ pf $\quad m = 0.1\text{-}0.4$

Some typical speed-density limiting values for various sources are listed in Table I. This table shows that even with high brightness dispenser cathodes ultrahigh density ($>10^9$ bits/in^2) and large bandwidth (> 10 MHz) cannot be attained with target readout. The assumed parameters for this conclusion are optimistic but attainable. To obtain greater than 10 MHz bandwidth, one must either trade bit density for higher speed or develop a high brightness Schottky emission source or a high-efficiency, secondary electron collection electron-optic system.

III. ELECTRON BEAM READOUT SENSITIVITY OF AMORPHOUS SEMICONDUCTOR THIN FILMS

The use of amorphous semiconductor thin films as the storage target in an electron beam memory has been described in the previous section. Two recording readout methods were described. One utilizes the inherent change in secondary yield between the amorphous and the crystalline phases and the second utilizes the change due to surface deformation. The possible advantages of the two methods were also described.

To determine quantitatively the possible modulation efficiency of recording by surface deformation mechanism, we have measured the angular dependence of secondary yields of amorphous semiconductor and Mo and have determined their roles in a simple theory of the modulation efficiency for this memory.

The readout signal from surface deformation is

$$I_s^\theta - I_s^o = (\delta_\theta - \delta_o)\, I_p \,. \tag{19}$$

Where I_s and I_p are the secondary and the primary electron beam currents; δ is the yield and θ and o indicate oblique and normal incidence. The readout modulation efficiency, m, can be defined as:

$$m = \frac{I_s^\theta - I_s^o}{I_s^o} \,. \tag{20}$$

A simplified theory for the modulation efficiency can be derived based upon Bruining's relationship for the yields, δ_θ and δ_o.[19] Based on some simplified assumption Bruining showed that[19]

$$\ln \frac{\delta_\theta}{\delta} = \alpha\chi_m(1-\cos\theta) \tag{21}$$

where α is the secondary electrons absorption coefficient and χ_m is the maximum depth from which secondary electron can escape the surface. Take the antilog of (21) and combine it with Eqs. (19) and (20) we find that the modulation efficiency is,

$$m = e^{k(1-\cos\theta)} - 1 \tag{22}$$

where we have defined the angular coefficient, $k = \alpha\chi_m$. The sensitivity of m to a change in angle is

$$\frac{dm}{d\theta} = e^{k(1-\cos\theta)}(k \sin\theta) \tag{23}$$
$$= (m+1)(k\sin\theta) \,.$$

Equation (22) shows that m is independent of the beam voltage if k is a constant. Previous investigations by Bruining on the angular dependence of δ of Ni and nickel carbide assumed k to be a constant.[19] The results were for beam voltage of less than 1 kV which is too low to be of interest for high density electron beam memory.

To evaluate k and thus m for amorphous semiconductors and Mo for voltages greater than 1 kV we have measured the angular dependence of δ of these materials. An apparatus with a rotatable sample stage suitable for the measurement of δ by the pulsed retarding potential method was used. It took place of the sample stage in our Electron Beam Test Cell. The schematic of the apparatus is shown in Fig. 16 and a photograph is shown in Fig. 17. To assure total collection of the emitted secondary electrons, the sample was biased (+90V) with the collector and the supporting structure grounded. For the high landing potentials, this bias introduced negligible error in our measurements. Low pulse rate (10 pps), short duration (14 μs) nanoampere electron beam excitation were used. The operating pressure was less than 5×10^{-8} torr.

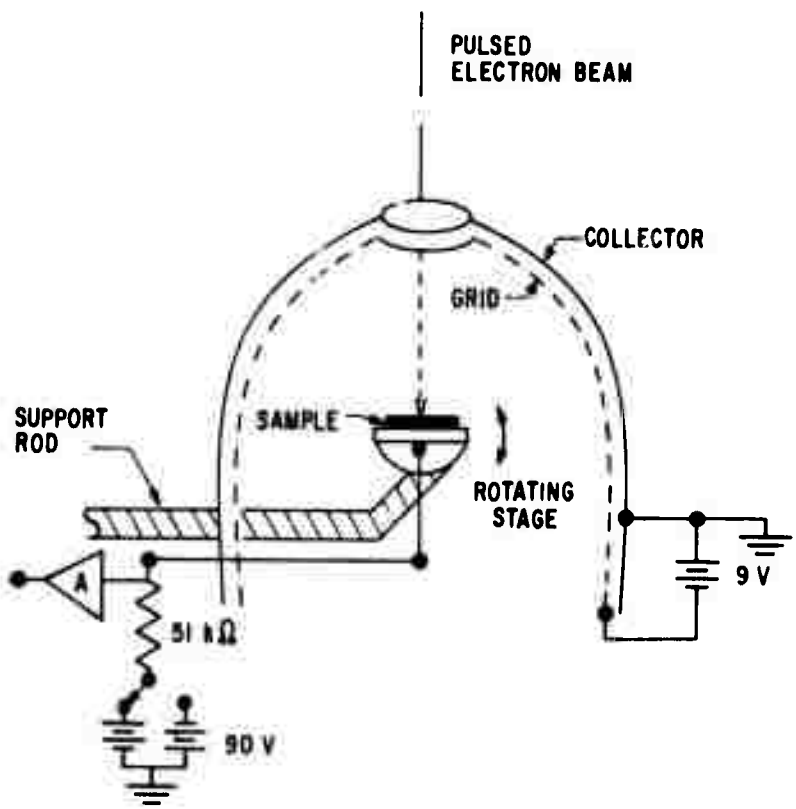

Figure 16 Schematic of the rotatable stage apparatus. The collector has been removed.

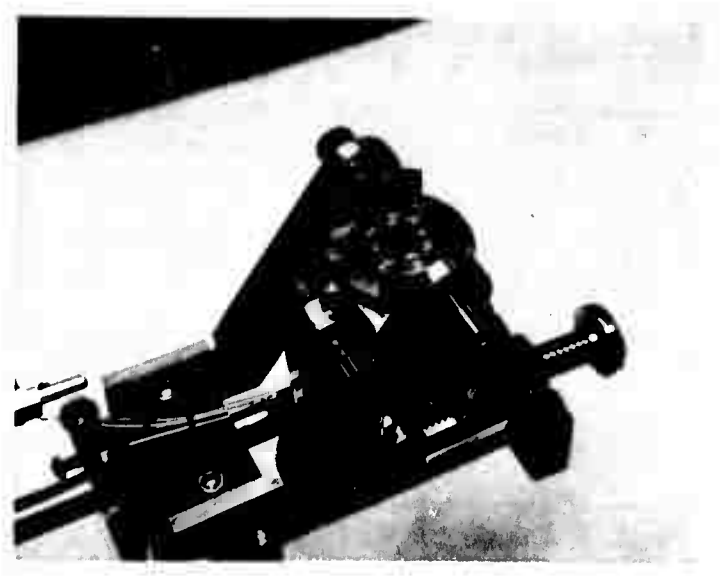

Figure 17 Photograph of the rotatable stage apparatus. The collector has been removed.

Thin film samples of 6000Å thick $Ge_{37}Te_{60}As_3$ and Mo were prepared by RF sputtering. The Ge-Te-As composition is of the irreversible switching composition[18] and showed almost identical secondary yield curve described in Ref. (18).

The crystalline form of $Ge_{37}Te_{60}As_3$ was obtained by heating the amorphous film to 300°C in an evaluated chamber. The crystallization temperature was determined by monitoring the sample resistance vs temperature. The measured crystallization temperature was approximately 235°C.

The assumed linear relationship between $\ln(\delta_\theta/\delta_0)$ vs $(1-\cos\theta)$, Eqn. (21), was verified by the measured yield vs angle of incidence.

A graph of the measured $\ln(\delta_\theta/\delta_0)$ vs $(1-\cos\theta)$ showed a straight line. Examples of this relationship for $Ge_{37}Te_{60}As_3$ in the amorphous form and Mo are shown in Figs. 18 and 19, respectively. Similar linear data points were measured for the crystalline form of $Ge_{37}Te_{60}As_3$.

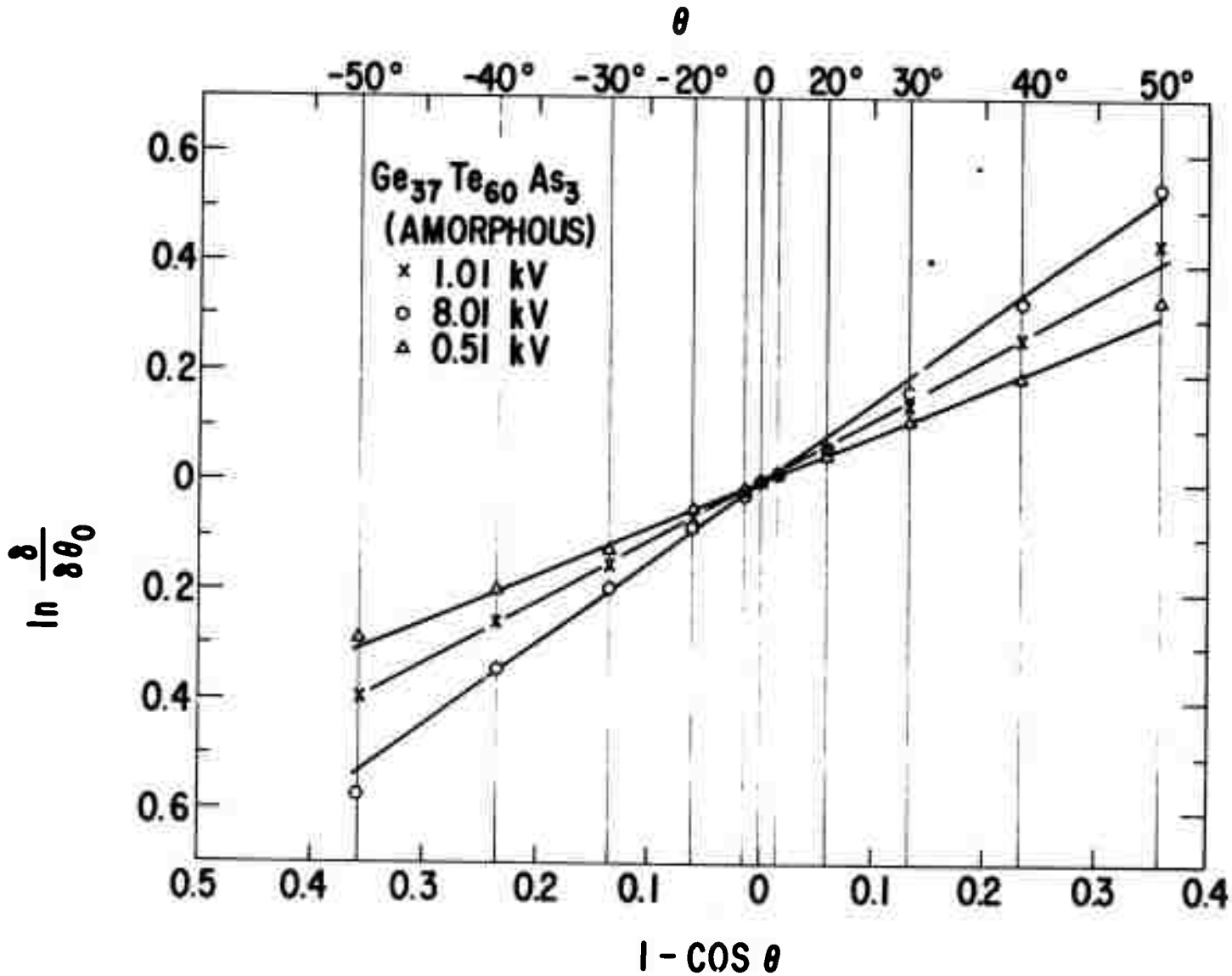

Figure 18 Measured $\ln(\delta_\theta/\delta_0)$ vs $(1-\cos\theta)$ for amorphous form of $Ge_{37}Te_{60}As_3$. θ is the angle of incidence.

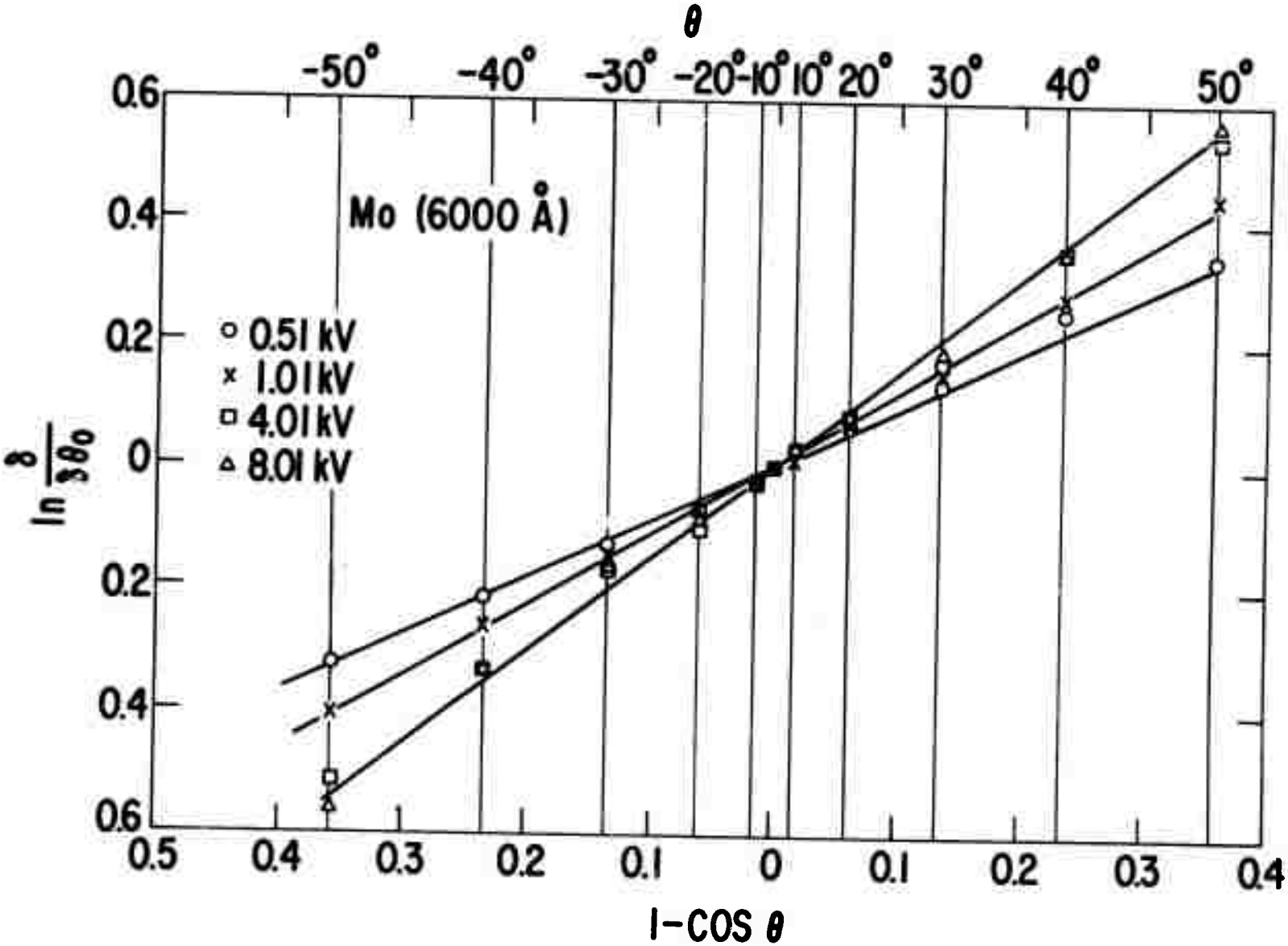

Figure 19 Measured $\ln(\delta_\theta/\delta_0)$ vs $(1-\cos\theta)$ for Mo.

However, the unexpected result is the change in the slope, k, with beam voltage. Both the crystalline and the amorphous form of $Ge_{37}Te_{60}As_3$ showed similar voltage dependence for their angular coefficient, k. This dependence is shown in Fig. 20. The measured angular coefficient of Mo had similar magnitude and voltage dependence and is shown in Fig. 21.

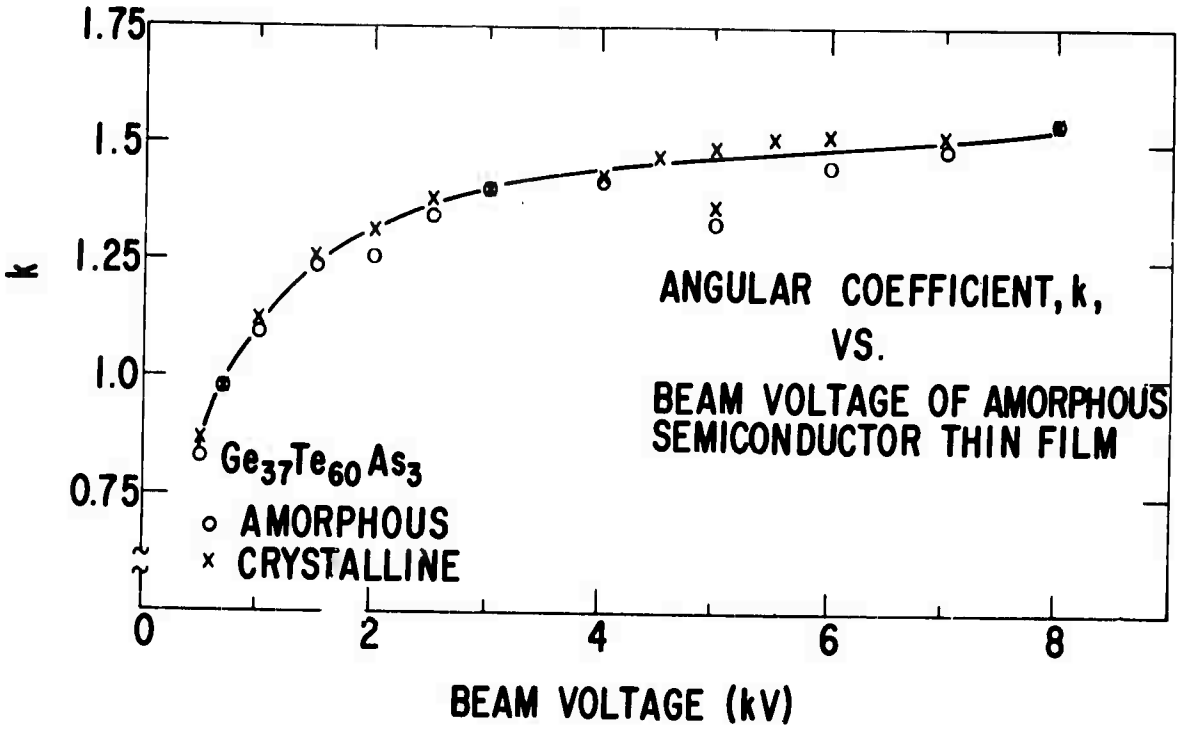

Figure 20 The angular coefficient, k, for amorphous and crystalline forms of $Ge_{37}Te_{60}As_3$ vs beam voltage.

With the measured angular coefficient and its voltage dependence, we are able to evaluate the possible modulation efficiency of amorphous semiconductors as an electron beam recording medium. We have plotted Eqn. (22) (Fig. 22) for some values of k applicable to amorphous semiconductors and Mo. For beam voltages between 1 to 8 kV, k lies between 1.1 to 1.6. Thus to obtain m of 20% requires a surface deformation of greater than 25°. With deformation of 45°--not an unreasonable number--m >50% is possible. One can speculate that to obtain high deformation angle requires a sharp and well defined electron beam profile as well as carefully controlled heating rate. To fulfill the above requirements so as to obtain a high modulation efficiency is the engineering challenge.

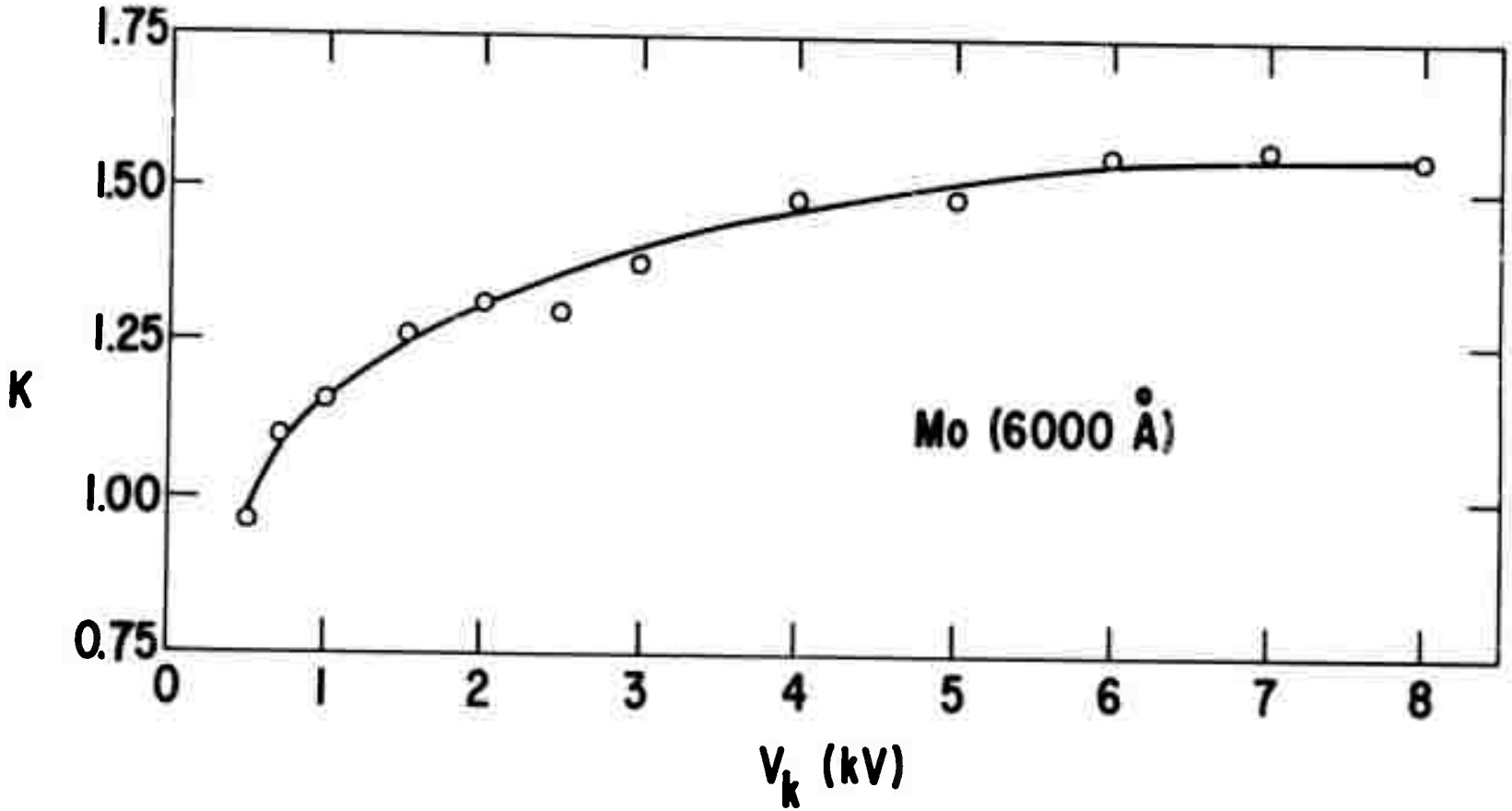

Figure 21 The angular coefficient, k, for Mo vs beam voltages.

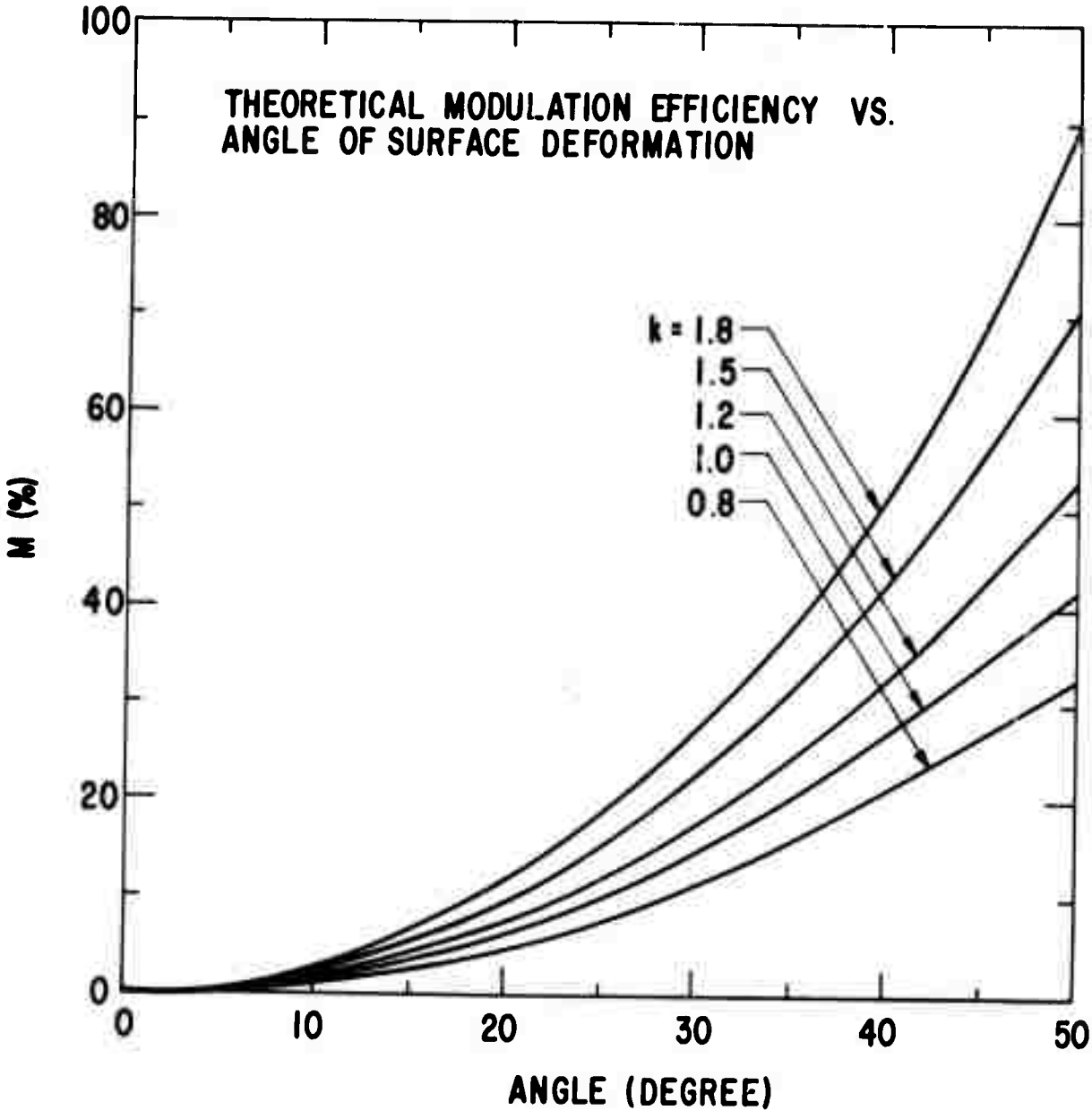

Figure 22 Theoretical modulation efficiency vs angle of surface deformation for some values of k.

IV. PARTICIPATING TECHNICAL PERSONNEL

A. C. M. Chen

A. M. Dunham

J. M. Wang

J. O. Fielding

REFERENCES

1. Session 23, Bulk Storage Systems, 1971 INTERMAG IEEE Trans. Mag., Vol. MAG-7, p. 830-848, December 1971.

2. S. P. Newberry, T. H. Klotz, and E. C. Buschmann, "Advances in Fly's Eye Electron Optics," Proc. of the National Electronics Conference, Vol. XXIII, p. 746-751, 1967.

3. A. C. M. Chen, J. F. Norton, and J. M. Wang, "Interaction of Electron Beam with Amorphous Semiconductor Thin Films," J. of Non-Crystalline Solids, Vol. 8-10, p. 917, 1971.

4. J. W. Weil, "Massive Stores--A Tutorial Introduction," Proc. of the 1971 Int. Computer Soc. Conference, p. 147-148, Sept. 1971.

5. R. B. Gentile and R. W. Grove, "Mass Storage Utility: Considerations for Shared Storage Applications," IEEE Trans. on Mag., Vol. MAG-7, p. 848, December 1971.

6. J. Dresner and G. B. Stringfellow, "Electronic Processes in the Photo-Crystallization of Vitreous Selenium," J. Phys. Chem. Solids, Vol. 29, p. 303 (1968).

7. J. Feinleib, J. deNeufville, S. C. Moss, and S. R. Ovshinsky, "Rapid Reversible Light-Induced Crystallization of Amorphous Semiconductors," Appl. Phys. Lett., Vol. 18, p. 254 (March 1971).

8. These recordings were made by J. E. Wolfe of the Electronics Laboratory, GE, Syracuse, New York.

9. L. G. Pittaway, "The Temperature Distributions on Thin Foil and Semi-infinite Targets Bombarded by an Electron Beam," Brit. J. Appl. Phys., 15, 967-982 (1964).

10. T. P. Lin, "Estimation of Temperature Rise in Electron Beam Heating of Thin Films, IBM J. of R&D, 11, 527-536 (1967).

11. J. A. Morrison and S. P. Morgan, "Electron Beam Heating of a Thin Film on a Highly Conducting Substrate," BSTJ, 45, 661-684 (1966).

12. E. J. Kobetich and R. Katz, "Energy Deposition by Electron Beams and X-rays," Phys. Rev. 170, 391-396 (1968).

13. "Thermophysical Properties of Matter, The TPRC Data Series," Ed. by Y. S. Touloukian and C. Y. Ho, IFI/Plenum, New York, 1970.

14. Properties of the 1173 Glass, Texas Instruments, Inc., P.O. Box 6015, M/S 561, Dallas, Texas 75222.

15. M. Sugi, S. Iizima, and M. Kikuchi, "Kinetics of Crystallization in Chalcogenide Glasses," J. of Non-Crystalline Solids, 5, 358-361 (1971).

16. No values are available for the chalcogenide glasses. However, they may be expected to have similar behavior as Silicon which has a total normal emittance of 0.3-0.6 between 251°-1000°K.

17. W.C. Hughes, "Long-life, High-Brightness Sources for Demountable Guns," 10th Symposium on Electron, Ion and Laser Beam Technology, Gaithersburg, Maryland, 21-23, May 1969, Ed. L. Marton.

18. A.C.M. Chen, J.F. Norton, and J.M. Wang, "Secondary Electron Emission of Amorphous Semiconductor Thin Films," Appl. Phys. Lett., Vol. 18, p. 443-444, May 1971.

19. J. Bruining, "The Depth at Which Secondary Electrons are Liberated," Vol. 3, p. 1046 (1936).

20. J.A. Savage, "Glass Forming Region and DTA Survey in the Ge-As-Te Memory Switching Glass System," J. of Mat. Sci., Vol. 6, p. 964-968, 1971.

21. P.F. Panter, "Modulation, Noise and Spectral Analysis," New York: McGraw Hill, 1965.

22. D.B. Langmuir, "Theoretical Limitation of Cathode Ray Tube," Proc. of IRE, Vol. 25, p. 977-991, Aug. 1937.

23. W.L. Hughes, "Current Distribution at the Focus of an Electron Lens with Spherical Aberration," Rpt. #68-C-264, GE R&D Center, July 1968.

24. A. van der Ziel, "Noise," Chap. 5, Prentice-Hall, Inc., Englewood, N.J., 1954.

25. T.E. Everhart, "Simplified Analysis of Point-Cathode Electron Sources," J. of Appl. Phys., Vol. 38, p. 4944-4957, Dec. 1967.